# Development of novel zinc ion-releasing glasses for conferring antibacterial activities to dental materials

Osaka University Graduate School of Dentistry

Course for Oral Science

(Department of Dental Biomaterials)

Supervisor: Professor Satoshi Imazato

**Fan Deng**

# ACKNOWLEDGEMENT

I would like to express my deepest gratitude to my supervisor, Professor Satoshi Imazato, Chair of the Department of Dental Biomaterials, Osaka University Graduate School of Dentistry, for his invaluable mentorship throughout my research. His academic wisdom has helped me overcome many challenges and successfully complete this thesis. Beyond his academic expertise, I deeply admire his ability to inspire and motivate, combined with generous support, creating a nurturing and stimulating environment, making this four-year journey both rewarding and memorable.

I also wish to express my sincere appreciation to Assistant Professor Haruaki Kitagawa for his significant contributions to my research. His dedication to my academic growth and willingness to provide constructive feedback at every stage of my research were indispensable. Additionally, his support and encouragement in my personal development have been a great source of inspiration.

My heartfelt thanks go to all the members in our department, not only for their kind assistance and collaboration during the research process, but also for their companionship and support in everyday life. The wonderful memories we have shared will be cherished as lifelong treasures.

Last but not least, I would like to extend my special thanks to my parents for their unwavering love and care, the capital I had to start life with, and on that capital I have made my way.

Fan Deng

# INDEX

# GENERAL INTRODUCTION

Oral diseases represent a significant proportion of the global disease burden, and continue to pose challenges to oral health professionals and individuals despite advancements in therapeutic strategies [1]. Most common oral infections, such as dental caries and pulpitis, are attributed to the disequilibrium of the oral microbial community [2]. Therefore, developing dental materials with antibacterial properties has become crucial for the effective control of bacteria.

Recently, several attempts have been made to provide ion-releasing glasses with antibacterial effects by incorporating zinc (Zn) [3-5]. $Zn^{2+}$ has multiple inhibitory effects on the physiology of intact bacterial cells, including glycolysis, ATPase activity, sugar phosphotransferase, and so on [6-8]. It can enhance proton permeability of bacterial cell membranes, reduce acid tolerance, and disrupt cell metabolism [9, 10]. However, trials to control ion release from the glasses to make it clinically effective, considering the usage conditions of dental materials, are limited.

In the engineering field, several technologies for soluble glasses are available [11-13]. Among them, silicate-based glass is known to dissolve in acids while it is relatively resistant to dissolution in neutral or slightly alkaline environments [14]. Tooth demineralization and subsequent early caries are normally caused by acid attacks from the acidogenic bacteria especially when there is plaque accumulation on the tooth surface [15]. Meanwhile, several kinds of bacteria which are called early colonizers

play a crucial role in shaping the composition and dynamics of the oral biofilm and are associated with maintaining homeostasis in the oral environment [16, 17]. Therefore, a prolonged expression of the antibacterial effects is not preferable from the perspective of maintaining oral health. Although antimicrobial properties are beneficial, there are concerns that they may be overexpressed beyond a necessary period. Based on these, it is expected that the acidity-responsive $Zn^{2+}$-releasing glass could achieve antimicrobial effects through the controlled and targeted release of $Zn^{2+}$ in response to pH fluctuation in the dental biofilm. Once the supragingival plaque forms on the surface of dental materials incorporating silicate-based glass containing Zn, it can be hypothesized that the release of $Zn^{2+}$ from the glass would be promoted by acids produced from the acidogenic bacteria, and thus inducing antimicrobial effects on demand in response to acidity (Figure 1).

On the other hand, phosphate-based glass dissolves rapidly under wet conditions regardless of the acidic/alkaline environment [18]. Delayed or inadequate treatment of early caries may allow it to progress beyond the enamel and into the dentin and even the pulp, increasing the likelihood of deep caries [19]. Selective (incomplete) caries removal is widely recommended for the treatment of deep caries, which involves the partial removal of carious dentin and leaving some affected dentin behind to avoid exposing the pulp [20, 21]. In addition to less invasive technique, the application of cavity liners or indirect pulp capping materials are often proposed to further protect the dentin and promote healing [22, 23]. One of the most popular liners and pulp-capping agents is calcium hydroxide ($Ca(OH)_2$), which is believed to exert antibacterial effects

through creating the local alkaline pH after dissolution [24, 25]. However, several studies have doubted the efficacy of $Ca(OH)_2$-based materials for the concern that the antibacterial effects are not strong enough to exhibit bactericidal effects in dentin [26, 27]. Since the risk from the remaining bacteria after selective caries removal cannot be ignored, it is necessary to strive for a sterile cavity. Therefore, in this study, it is hypothesized that the rapidly soluble $Zn^{2+}$-releasing glass could quickly release high concentration of $Zn^{2+}$ and exhibit cavity disinfecting effects (Figure 2).

Overall, by utilizing these glass technologies, it is considered possible to fabricate $Zn^{2+}$-releasing glasses that enable dental resins to exhibit antibacterial effects on demand in response to acidity or resin-based liners to exert immediate cavity disinfecting effects.

# OBJECTIVES AND CONTENTS

The purpose of this study was to develop two different types of glass particles; acidity-responsive $Zn^{2+}$-releasing glass and rapidly soluble $Zn^{2+}$-releasing glass, and to evaluate their ion releasing properties and antibacterial effects. Additionally, dental resins incorporating each glass were fabricated and their effectiveness was investigated.

In experiment 1, the acidity-responsive $Zn^{2+}$-releasing glass was fabricated using silicate glass technology, followed by assessments of physicochemical characteristics and antibacterial properties *in vitro.* Then, it was incorporated into dental resins and the antibacterial ability was examined.

In experiment 2, the rapidly soluble $Zn^{2+}$-releasing glass was fabricated using phosphate glass technology and characterized, and its bactericidal effect against oral bacteria was evaluated. Then, it was incorporated into dental resins and the antibacterial ability against bacteria in dentinal tubules was examined.

# EXPERIMENT 1

# Fabrication of acidity-responsive $Zn^{2+}$-releasing glass and incorporation into dental resins

## 1.1 Materials and methods

### 1.1.1 Fabrication of acidity-responsive $Zn^{2+}$-releasing glasses (AGs)

Three types of acidity-responsive silicate-based glasses containing Zn (AGs) were fabricated by melt-quenching method [28] and coded as AG-1, AG-2, and AG-3 in ascending order of Zn content. Briefly, silicon dioxide ($SiO_2$), sodium carbonate ($Na_2CO_3$), zinc oxide (ZnO), zinc fluoride tetrahydrate ($ZnF_2 \cdot 4H_2O$), purchased from FUJIFILM Wako Pure Chemical Corporation (Osaka, Japan), were mixed and melted in a platinum crucible at 1300℃ (AG-1 and AG-2) or 1350℃ (AG-3) for 1 hour. The melted glass was quenched in water bath at room temperature and pressed by an iron plate to obtain glass cullet. After drying at 110℃ for 5 hours, the glass cullet was ground into particles with a planetary ball mill machine (PULVERISETTE 5/4, Fritsch, Germany). The particles that were not sufficiently ground were excluded by passing them through a stainless-steel sieve (250-μm mesh testing sieve, Nonaka Rikaki, Tokyo, Japan). The mixing ratios of components for glass preparation are listed in Table 1. A silicate-based glass powder (BioUnion filler) used for a commercially available glass-ionomer cement (Caredyne Restore, GC corp., Tokyo, Japan) was used as the control glass (Cont). All the glass particles were sterilized with ethylene oxide gas.

### 1.1.2 Characterization of AGs

High-resolution imaging of the AG surfaces and their elemental mapping were obtained by field emission scanning electron microscopy (FE-SEM; JSM-F100, JEOL, Tokyo, Japan) and energy dispersive spectroscopy (EDS; JSM-F100, JEOL). The glass structure was observed by an X-ray diffraction detector (XRD; PIXcel$^{1D}$, Malvern Panalytical Ltd., Worcestershire, UK). The size distribution of glass particles was measured by a particle size analyzer (Partica LA-960V2, Horiba, Kyoto, Japan). Further, the elemental composition of each glass was analyzed by X-ray fluorescence (XRF; ZSX Primus IV$i$, Rigaku, Tokyo, Japan).

### 1.1.3 Evaluation of solubility and ion-releasing property of AGs

The solubility of AGs in the buffer solution at pH 7.0, 6.0, or 5.0 was evaluated. The buffer solution was prepared by 4-(2-hydroxyethyl)-1-piperazineethanesulfonic acid (HEPES; FUJIFILM Wako Pure Chemical) and acetate buffer (Kanto Chemical, Tokyo, Japan). Fifty mg of each glass was immersed in 10 mL of each buffer solution. After 100-rpm gyratory shaking at 37℃ for 24 hours, the suspensions were filtered through a glass fiber filter with a pore size of 0.5 μm (ADVANTEC, Tokyo, Japan) which was weighed beforehand. The glass fiber filter with the undissolved glass was dried at 110°C for 6 hours and the total weight was measured. The solubility was obtained by calculation. The experiment was repeated three times.

Release of $Zn^{2+}$ and $F^{-}$ from each glass into pH-adjusted Brain Heart Infusion (BHI) broth (Becton Dickinson, Maryland, USA) were evaluated. The pH of BHI broth was

adjusted by adding 1 mol/L hydrochloride acid (HCl; Kanto Chemical) until reaching the value of 7.0, 6.0, or 5.0. Twenty mg of each glass was placed in a well of a 96-well microplate, and 200 μL of pH-adjusted BHI broth was poured into the wells containing glass particles. After 100-rpm gyratory shaking at 37℃ for 24 hours, the suspensions were passed through a 0.22 μm syringe filter (Merck Millipore Ltd., Carrigtwohill, Ireland), and diluted with 9.8 mL of distilled water. The dilutions were used for determining the concentration of $Zn^{2+}$ with an inductively coupled plasma-optical emission spectrometer (ICP-OES; iCAP7200 ICP-OES Duo, Thermo Fisher Scientific, Cambridge, UK), as well as the concentration of $F^-$ with a fluoride ion electrode (FIE; 6561S-10C, Horiba). The experiment was repeated five times.

### 1.1.4 Bacteria used

*Streptococcus mutans* NCTC10449 from a stock culture was cultured in BHI broth and on BHI agar (Becton Dickinson) plates at 37°C for 24 hours under an anaerobic condition and used for the following experiments.

### 1.1.5 Measurements of MICs and MBCs of $Zn^{2+}$ and $F^-$ against *S. mutans*

To evaluate the concentrations of $Zn^{2+}$ and $F^-$ that could effectively inhibit the growth of *S. mutans*, the minimum inhibitory concentrations (MICs) and minimum bactericidal concentrations (MBCs) of each ion were measured with a broth dilution method [29]. Zinc nitrate ($Zn(NO_3)_2$; FUJIFILM Wako Pure Chemical) and sodium fluoride (NaF; FUJIFILM Wako Pure Chemical) were used for standard solutions of $Zn^{2+}$ and $F^-$,

respectively. Fifty μL of standard solutions with a concentration of 32.5 – 1000 ppm obtained after serial two-fold dilutions were poured into the wells of a 96-well microplate. Fifty μL of *S. mutans* suspensions, adjusted to approximately $2 \times 10^6$ CFU/mL in double-concentration BHI broth, were poured into each well containing the standard solutions to prepare 16.25 – 500 ppm of Zn solutions with $1 \times 10^6$ CFU/mL of bacterial suspensions. After anaerobic incubation at 37°C for 24 hours, the turbidity of the suspensions was observed visually, and the MIC, which is the lowest concentration that prevents visible bacterial growth, was determined. Twenty μL of the samples with no visible turbidity were inoculated on BHI agar plates. After anaerobic incubation at 37°C for 48 hours, the MBC, which is the lowest concentration of the agent that kills the bacterium, was determined using the agar plates with no bacterial colonies. The experiment was repeated five times.

### 1.1.6 Evaluation of antibacterial activity of AGs

The *S. mutans* suspension was adjusted to approximately $1 \times 10^6$ CFU/mL in BHI broth, and the pH of the bacterial suspension was adjusted to the value of 7.0, 6.0, or 5.0 by adding 1 mol/L HCl. A total of 20 mg of each glass was placed in a well of a 96-well microplate, and 200 μL of pH-adjusted *S. mutans* suspension was poured into the wells containing glass particles. After anaerobic incubation at 37°C for 24 hours with gyratory shaking at 100 rpm, 100 μL of the suspension was collected and diluted with 9.9 mL of BHI broth. The suspension was serially diluted with BHI broth and 100 μL of the dilutions were inoculated on BHI agar plates. The plates were incubated

anaerobically at 37°C for 48 hours, after which the number of forming colonies was counted. The experiment was repeated five times.

### 1.1.7 Evaluation of on-demand ion-releasing property of AGs

A total of 20 mg of Cont, AG-2, or AG-3 was placed in a well of a 96-well plate and immersed in 200 μL of acetate buffer (pH 5.0) at 37°C for 1 day. Then, the solution was replaced by 200 μL of HEPES (pH 7.0) for 3 days while being exchanged every 24 hours. This procedure was repeated until Day 9, so that the third exposure of glass to acetate buffer was completed. That is, the glasses were immersed in acetate buffer on Days 0 – 1, 4 – 5 and 8 – 9 and in HEPES on Days 1 – 4 and 5 – 8. During this period, 100 μL of the eluates were collected every 24 hours and diluted with 9.9 mL of distilled water. The concentrations of $Zn^{2+}$ in the dilutions were measured by using ICP-OES. The experiment was repeated three times (Figure 3).

### 1.1.8 Evaluation of on-demand antibacterial activity of AGs

The particles of Cont, AG-2, or AG-3 were collected on Day 8 (after two-cycle exposures to acetate buffer and HEPES) using the same method as described in 1.1.7. The concentration and pH value of *S. mutans* suspension were adjusted to approximately $1 \times 10^6$ CFU/mL, and pH 7.0 or 5.0, respectively. The glass particles were immersed in 200 μL of pH-adjusted *S. mutans* suspension. After anaerobic incubation at 37°C for 24 hours with gyratory shaking at 100 rpm, 100 μL of the suspension was collected and diluted with 9.9 mL of BHI broth. The suspension was

serially diluted with BHI broth, and 100 μL of the dilutions were inoculated on BHI agar plates. The plates were incubated anaerobically at 37°C for 48 hours, after which the number of forming colonies was counted. The bacterial suspension without any glass was used for comparison. The experiment was repeated three times (Figure 4).

### 1.1.9 Fabrication of dental resins incorporating AG

The experimental resin was prepared by mixing AG-3 with triethylene glycol dimethacrylate (TEGDMA), 2-hydroxyethyl methacrylate (HEMA), camphorquinone (CQ), ethyl *p*-dimethylaminobenzoate (EPA), and 2,6-di-tert-butyl-*p*-benzoyl (BHT) (Table 2). The particles of AG-3 and the liquid of uncured resin were mixed in a ratio of 1:9, 2:8, or 3:7 (w/w), providing 10, 20, or 30 (wt)% AG-3 in the experimental resins. The mixture was dropped into a polytetrafluoroethylene circular ring mold (7 mm diameter, 1 mm thickness), pressed with a celluloid strip and glass slide, and followed by 60-second light-curing (Pencure 2000, Morita, Kyoto, Japan) with the light intensity of 2,000 mW/cm$^2$. The specimens were polished using silicate carbide grinding papers (#120 to #2000; Buehler, Lake Bluff, IL, USA) and sterilized by ethylene oxide gas. The cured resin without AG-3 was used as a control (Cont).

### 1.1.10 Evaluation of antibacterial activity of dental resins incorporating AG

On-disc culture assay was conducted to evaluate the antibacterial activity of the experimental resins incorporating 10, 20, and 30 (wt)% AG-3. Twenty μL of the pH-adjusted *S. mutans* suspension (pH 7.0, 6.0, or 5.0) with a concentration of

approximately $1 \times 10^6$ CFU/mL was inoculated on the surface of each specimen. After anaerobic incubation at 37°C for 24 hours, 10 μL of the suspension was collected and poured into 990 μL of BHI broth. The suspension was serially diluted with BHI broth, and 100 μL of the dilutions were inoculated on the BHI agar plates. The plates were incubated anaerobically at 37°C for 48 hours, after which the number of forming colonies was counted. The experiment was repeated three times.

### 1.1.11 Evaluation of on-demand ion-releasing property of dental resin incorporating AG

The experimental resin incorporating 30 (wt)% AG-3 was exposed to acetate buffer and HEPES using the same method as described in 1.1.7. During the experiment, 100 μL of the eluates were collected every 24 hours and diluted with 4.9 mL of distilled water. The concentrations of $Zn^{2+}$ in the dilutions were measured by using ICP-OES. The experiment was repeated three times.

The surface of the experimental resin before exposure to buffer solution (Day 0) and after the third exposure to acetate buffer (Day 9) was observed by SEM (JSM-6510LV, JEOL) at 30 kV and magnifications of ×200 or ×1000.

### 1.1.12 Evaluation of on-demand antibacterial activity of dental resin incorporating AG

The experimental resin incorporating 30 (wt)% AG-3 was exposed to acetate buffer and HEPES using the same method as described in 1.1.7. On Day 8 (after two-cycle

exposures to acetate buffer and HEPES), the specimens were rinsed in distilled water and placed in a sterile environment until dried. Twenty μL of the pH-adjusted *S. mutans* suspension (pH 7.0, or 5.0) with a concentration of approximately $1 \times 10^6$ CFU/mL was inoculated on the specimen surface. After anaerobic incubation at 37°C for 24 hours, 10 μL of the suspension was collected and poured into 990 μL of BHI broth. The suspension was serially diluted with BHI broth and 100 μL of the dilutions were inoculated on the BHI agar plates. The plates were incubated anaerobically at 37°C for 48 hours, after which the number of viable bacteria was counted (Figure 5). The experiment was repeated three times.

### 1.1.13 Evaluation of anti-biofilm effects of dental resin incorporating AG

Human unstimulated saliva was collected from 4 healthy subjects (2 male and 2 female) aged 25 – 35 years (mean 30.0 ± 4.4 years). No clinical signs of caries, gingivitis, or periodontitis were detected, and no systemic disease was observed in any of the subjects. This experiment was approved by the Ethics Review Committee of Osaka University Graduate School of Dentistry and Osaka University Dental Hospital (Approval number: R1-E52). The collected saliva was filtered twice with a 0.22 μm syringe filter (Merck Millipore Ltd.).

The experimental resin incorporating 30 (wt)% AG-3 was exposed to acetate buffer and HEPES using the same method as described in 1.1.7. On Day 9, after the third exposure to acetate buffer, the specimens were collected and immersed in 1 mL of filtered saliva for 2 hours. Then, the specimens were transferred to the wells containing

200 μL of *S. mutans* suspension ($1 \times 10^6$ CFU/mL) in a 48-well microplate. After 12 hours, the specimens were transferred into new wells containing 200 μL of BHI broth supplemented with 2% sucrose (FUJIFILM Wako Pure Chemical) for 20 minutes, followed by 6-hour immersion in BHI broth. The alternate immersion into BHI broth with or without sucrose was conducted again. After the third 20-minute immersion in BHI broth with 2% sucrose, the specimens were gently rinsed in 200 μL of phosphate buffered saline (PBS; FUJIFILM Wako Pure Chemical). All the procedures were conducted at 37℃ under an anaerobic condition (Figure 6). The cured resin without AG-3 was used as a control.

To observe the morphological feature of biofilm adhered to the specimens, the cellular structures were fixed by sequentially storing them in 0.1 M cacodylic acid (FUJIFILM Wako Pure Chemical) for 20 minutes, 0.1 M half-karnovsky solution (FUJIFILM Wako Pure Chemical) for 30 minutes, and 0.1 M cacodylic acid for 45 minutes at 4°C. The specimens were gradually dehydrated through sequentially being immersed in ethanol for 20 minutes with increasing concentrations: 50%, 70%, 80%, 90%, 96%, and 99.5%, followed by freeze-drying for 60 minutes in the freeze-drying machine (JFD-320, JEOL). After dehydration, the specimens were coated with gold (QUICK COATER SC-701, Sanyu Electron, Tokyo, Japan) and observed by SEM (JSM-6510LV, JEOL) at 30 kV and ×2000 magnification.

The biofilm formed on the specimen surface was stained using LIVE/DEAD™ BacLight™ bacterial viability kits (L7007, Molecular Probes, Eugene, OR, USA) according to the manufacturer's instructions. Briefly, 2 μL of component A (SYTO 9

dye, 1.67 mM/ propidium iodide, 1.67 mM solution in DMSO) and 2 μL of component B (SYTO 9 dye, 1.67 mM/ propidium iodide, 18.3 mM solution in DMSO) were mixed in 1 mL of distilled water. A hundred μL of the mixed solution was dropped on the specimens and incubated at 37°C for 15 minutes under the dark condition. After gently irrigating with distilled water, the specimens were visualized using a confocal laser scanning microscope (CLSM; LSM 700, Carl Zeiss, Oberkochen, Germany) at 488 and 555 nm for excitation, and 500 and 635 nm for emission. The images were obtained using a ZEN Imaging Software (Carl Zeiss). A preliminary image was taken to determine the acquisition parameters and the setting was kept constantly for all images. Scans were taken in 12 bits at a resolution of 1024 by 1024 with the following setting: Speed = 8; Pinhole size = 34 μm; Digital offset = 0; Master gain (Ch1, SYTO 9) = 493; Master gain (Ch2, propidium iodide) = 706. Three images were obtained from one sample, and the images were analyzed by Imaris software (Bitplane, Zurich, Switzerland) to determine the thickness of biofilm and the percentage of membrane-compromised cells. The experiment was repeated three times.

### 1.1.14 Statistical analysis

Statistical analyses were performed using SPSS Statistics 25 (IBM, Chicago, IL, USA). The homogeneity of variances was confirmed initially. The results of solubility, cc release, bacterial growth, on-demand bacterial growth, bacterial growth on the experimental resin were statistically analyzed by the analysis of variance (ANOVA) and Tukey's honestly significant difference (HSD) test. $p < 0.05$ was considered to

indicate significance in this study. The results of on-demand bacterial growth inoculated on the experimental resin, the thickness of biofilm and the percentage of membrane-compromised cells in the biofilm were analyzed by student's *t*-test with a significance level of $p < 0.05$.

## 1.2 Results

### 1.2.1 Characteristics of AGs

The FE-SEM images of the experimental glass particles are shown in Figure 7. All glasses were in irregular shapes and confirmed to be amorphous based on the XRD patterns shown in Figure 8. The size distribution of each glass particle is shown in Figure 9. The median diameter of AG-1, AG-2, and AG-3 was approximately 11.3, 10.9, and 11.3 μm, respectively. No remarkable difference was observed in the particle size range and distribution amongst the three glasses.

By XRF analysis, $SiO_2$, ZnO, $Na_2O$ and F were detected in AG-1 with 42.9, 25.3, 7.1, and 17.0%, in AG-2 with 33.4, 34.6, 7.8, and 16.0%, and in AG-3 with 29.2, 42.7, 9.2, and 10.5%, respectively (Table 3). No remarkable difference in composition was observed between the preparation and the results of XRF analysis.

The elemental mapping images revealed that the elements were evenly dispersed in the glass particles, and the concentration of $Zn^{2+}$ increased from AG-1 to AG-3 (Figure 10).

### 1.2.2 Solubility and ion-releasing property of AGs

Figure 11 shows the solubility of each glass particle in the pH-adjusted buffer solution (pH 7.0, 6.0, or 5.0). When the pH value decreased, the solubility of each glass significantly increased ($p < 0.05$, ANOVA, Tukey's HSD test). Across all the pH conditions, AG-3 showed the greatest solubility while Cont showed the lowest solubility.

The concentrations of $Zn^{2+}$ and $F^-$ released from each glass into the pH-adjusted BHI broth (pH 7.0, 6.0, or 5.0) are shown in Figure 12. With a decrease in pH values, the release of $Zn^{2+}$ from Cont, AG-1, AG-2, and AG-3 increased significantly ($p < 0.05$, ANOVA, Tukey's HSD test). When the pH condition was at 5.0, the release of $Zn^{2+}$ significantly increased in the order of Cont, AG-1, AG-2, and AG-3. The release of $F^-$ from Cont significantly increased ($p < 0.05$, ANOVA, Tukey's HSD test) with pH decrease. AG-2 and AG-3 released less $F^-$ under acidic conditions (pH 6.0, 5.0) than under the neutral condition (pH 7.0) while AG-1 released more $F^-$ under acidic conditions than under the neutral condition. Under each pH condition, AG-3 released the least $F^-$ while Cont released the most $F^-$.

### 1.2.3 MICs and MBCs of $Zn^{2+}$ and $F^-$ against *S. mutans*

For $Zn^{2+}$, the MIC and MBC against *S. mutans* were 125 and 250 ppm, respectively. For $F^-$, the MIC against *S. mutans* was 125 ppm, whereas the MBC was greater than 500 ppm.

### 1.2.4 Antibacterial activity of AGs

Figure 13 shows the number of viable bacteria after incubating the pH-adjusted *S. mutans* suspension in the presence of Cont, AG-1, AG-2, and AG-3. The colony counts of viable *S. mutans* demonstrated a significant decrease with the pH decrease for all the groups ($p < 0.05$, ANOVA, Tukey's HSD test). No significant difference was found in the number of surviving cells between Cont and without glass particles when the pH value was at 7.0 or 6.0, neither was between AG-1 and AG-2. Except for Cont, the viable bacterial number after incubating with AG-1, AG-2, and AG-3 was significantly smaller than that without any glass particles under each pH condition. When the pH value was at 5.0, the bacterial number significantly decreased with the increased content of Zn in the glasses. Among all the groups, the number of bacteria in the presence of AG-3 was the lowest under all conditions. The number of viable cells in the presence of AG-2 (pH 5.0) and AG-3 (pH 6.0 and 5.0) was significantly smaller than the initial number of bacteria (approximately $1 \times 10^6$ CFU/mL), indicating that AG-2 and AG-3 exhibited bactericidal effects at the corresponding pH values.

### 1.2.5 On-demand ion-releasing property of AGs

Figure 14 shows the concentration of $Zn^{2+}$ released from Cont, AG-2, and AG-3 with repeated exposures to acetate buffer and HEPES. On Day 1, the concentration of $Zn^{2+}$ released from Cont, AG-2, and AG-3 was 205.8 ± 10.5, 359.6 ± 12.5, and 408.2 ± 17.7 ppm, respectively. The amount of released $Zn^{2+}$ under the neutral condition on Days 2 – 4 and 6 – 8 decreased dramatically, which was less than 80 ppm. When the tested

glasses were again immersed in acetate buffer on Days 5 and 9, the amounts of released $Zn^{2+}$ increased accordingly and reached the same levels as that on Day 1.

### 1.2.6 On-demand antibacterial activity of AGs

Figure 15 shows the number of viable *S. mutans* after incubating in the presence of Cont, AG-2, and AG-3 before and after two-time exposures to acetate buffer and HEPES. No significant differences were observed for the number of bacteria in the presence of AG-2 and AG-3 before and after exposures at pH 5.0 ($p > 0.05$, ANOVA, Tukey's HSD test). Further, the number of viable cells in the presence of AG-2 and AG-3 at pH 5.0 after repeated exposures was significantly smaller than those in the presence of Cont and the initial number of bacteria ($p < 0.05$, ANOVA, Tukey's HSD test). Compared with the number of bacteria in the presence of AG-2, AG-3 exhibited greater inhibition of *S. mutans* at pH 5.0 ($p < 0.05$, ANOVA, Tukey's HSD test).

### 1.2.7 Antibacterial activity of dental resins incorporating AG

Figure 16 shows the number of viable *S. mutans* after incubation on the surface of dental resins incorporating 10, 20, or 30 (wt)% AG-3. At pH 5.0 and 6.0, the number of viable cells on the experimental resin incorporating 30 (wt)% AG-3 was significantly smaller than those on both the control and the experimental resins incorporating 10 and 20 (wt)% AG-3 ($p < 0.05$, ANOVA, Tukey's HSD test). This reduction was also significant compared to the initial amount of bacteria, indicating that the experimental resin incorporating 30% AG-3 exhibited bactericidal effects under acidic conditions.

### 1.2.8 On-demand ion-releasing property of dental resin incorporating AG

The concentration of $Zn^{2+}$ released from dental resin incorporating 30 (wt)% AG-3 with repeated exposures to acetate buffer and HEPES is shown in Figure 17. The concentrations of $Zn^{2+}$ released increased repeatedly in response to exposure to acids. On Day 1, the concentration of $Zn^{2+}$ released from the specimens was 354.0 ± 27.4 ppm. The amount of released $Zn^{2+}$ under neutral condition on Days 2 – 4 and 6 – 8 decreased dramatically, to 16.5 ± 4.3 and 9.1 ± 2.2 ppm (mean ± S.D.), respectively. When the experimental resin was again immersed in acetate buffer, the amount of $Zn^{2+}$ released on Days 5 and 9 increased to 317.8 ± 23.2 and 345.8 ± 81.8 ppm, respectively. There was no significant difference among the released $Zn^{2+}$ amount when the specimen was exposed to acidic conditions on Days 1, 5 and 9 ($p > 0.05$, ANOVA, Tukey's HSD test).

SEM observation confirmed that the AG-3 particles remained well-integrated in the experimental resin, with no substantial alterations in the surface morphology even after repeated acidic exposures (Figure 18).

### 1.2.9 On-demand antibacterial activity of dental resin incorporating AG

Figure 19 shows the number of viable *S. mutans* after incubation on the surface of dental resin incorporating 30 (wt)% AG-3 before and after two-time exposures to acetate buffer and HEPES. After exposures, the amount of viable *S. mutans* on the resin incorporating 30 (wt)% AG-3 at pH 5.0 was significantly smaller than that at pH 7.0 ($p < 0.05$, student's *t*-test). The viable bacterial amount at pH 5.0 was smaller than the initial amount, indicating that killing effects of the experimental resin were maintained.

### 1.2.10 Evaluation of anti-biofilm effects of dental resin incorporating AG

Figure 20 shows the representative SEM images of the biofilms formed on the control resin without AG-3 and the dental resin incorporating 30 (wt)% AG-3 after repeated exposures to acetate buffer and HEPES. In the biofilm adhered to the experimental resin, less density of bacteria and extracellular matrix were observed compared with the control resin. On the experimental resin, the morphology of the bacteria was observed to be disrupted (arrow).

Figure 21 displays the thickness of biofilm (A) and the percentage of membrane-compromised bacteria (B) analyzed from the CLSM images of *S. mutans* biofilm formed on the control resin without AG-3 and the dental resin incorporating 30 (wt)% AG-3 after repeated exposures to acetate buffer and HEPES. In comparison with the control resin, the surface of the experimental resin exhibited a significantly thinner biofilm ($p < 0.05$, student's *t*-test). A higher percentage of membrane-compromised cell was observed on the experimental resin as compared with the control resin ($p < 0.05$, student's *t*-test).

## 1.3 Discussion

Recently, several attempts have been made to provide ion-releasing glasses with antibacterial effects by replacing certain components with metals such as silver (Ag), copper (Cu), or Zn, thereby exhibiting strong antibacterial properties [30-33]. Among them, Ag- and Cu-doped silicate-based glasses have been extensively studied because

of their ability to inhibit the microorganisms [34-36]. However, one of the major issues in incorporating Ag- and Cu-doped glasses into dental resins is discoloration [37, 38]. To overcome this issue, the potential of usage of Zn to minimize the discoloration has been investigated [39-41]. In addition, as an essential trace element for human body, the usage of Zn is more advantageous than Ag and Cu due to the superior biocompatibility of Zn, whose cytotoxicity was proved to be the least among the three metal ions [42, 43].

BioUnion filler used for a commercially available glass-ionomer cement (Caredyne Restore) is a silicate-based glass powder composing of $SiO_2$, ZnO, CaO, and F that is capable of releasing $Zn^{2+}$, $Ca^{2+}$, and $F^-$ [44]. Liu *et al.* [45] reported that the release of $Zn^{2+}$ from BioUnion filler was accelerated under acidic conditions. Such acidity-induced release of $Zn^{2+}$ from BioUnion filler effectively inhibited *S. mutans*. This technology enables the on-demand release of antimicrobial components from dental materials. However, the effects of BioUnion filler were not bactericidal effects even when the initial bacterial amount was at a relatively low level. On this basis, in this study, three types of experimental silicate-based glasses containing Zn were designed without the addition of Ca, replacing Ca in BioUnion filler with Zn to enhance antibacterial activity. Therefore, BioUnion filler was used as the control glass (Cont) in this study, consistently comparing the result of these new glasses and BioUnion filler to evaluate the enhancement in antibacterial properties.

Dental caries is a disease caused by a dental plaque (syn. an oral biofilm) formed on tooth surfaces and a pH-decrease in the plaque with an intake of carbohydrate. In

the supragingival plaque, the pH is normally maintained in the range of 6.7-7.3 by a perfusion of saliva with the capacity of pH-buffering [46]. A critical pH at which enamel demineralization occurs is 5.2-5.5 [47]. Due to the gingival recession and root surface exposure, caries frequently occurs on the root surface especially in the elderly. Since the cementum and dentin exposed on the root surface have lower acid resistance than enamel, the critical pH of cementum has been reported to be in the range of 6.2-6.7 [48, 49]. Therefore, in this study, the solubility and ion release of the glasses were tested in buffers/medium with pH 5.0, 6.0, or 7.0, and the pH of bacterial suspensions was also adjusted to the same levels.

Due to the field strength falling between the network modifier and intermediate oxide, $Zn^{2+}$ behaves either as a modifier or network former in glasses [50]. As a modifier, $Zn^{2+}$ exists as charged single ions among the cross-linked glass network [51]. It disrupts the regular bonding between the glass-forming components and oxygen through non-bridging oxygen (NBO; Si-O-$M^{+}$, where $M^{+}$ is a modifier ion). This decreases the relative quantity of strong bonds in the glass. As a network-former, $Zn^{2+}$ enters the silicate network by forming Si-O-Zn bonds. The mechanism of glass dissolution involves the ion exchange (protons for modifier ions) and acid hydrolysis of Si-O-Zn bonds. It has been confirmed that $Zn^{2+}$-releasing silicate-based glasses were stable at physiological pH but showed accelerated dissolution under acidic conditions [52]. This suggested that Zn enters the silicate network to a much greater extent, with a majority or potentially all of Zn forming Si-O-Zn bonds [51]. By comparing these findings with previous studies, it is evident that adding ZnO to silicate-based glasses

can modify ion-releasing behavior in response to changes in the pH environment. Consequently, the glasses are more stable at neutral pH levels but quickly dissolve under acidic conditions. In this study, the solubility of glass particles in acids and the release of $Zn^{2+}$ increased with an increase in the Zn content. Additionally, all glasses dissolved more greatly and released a greater amount of $Zn^{2+}$ with a decrease in pH. These results can be attributed to the degradation mechanisms discussed above, where a higher amount of Zn content is related to higher NBO and Si-O-Zn bonds in the glass structure, thus releasing a larger amount of $Zn^{2+}$ in aqueous solution, particularly under acidic conditions.

BioUnion filler (Cont) showed the greatest amount of $F^-$ release among the four groups despite the equivalent preparation of F. With the increase of Zn in the glass (Cont < AG-1 < AG-2 < AG-3), the release of $F^-$ from the glass decreased (Cont > AG-1 > AG-2 > AG-3). While the $Zn^{2+}$ release increased with pH decrease, $F^-$ release under acidic conditions from each AG was significantly lower than under the neutral pH condition. This may be explained by the complexing reaction: $Zn^{2+} + HF \rightarrow ZnF^+ + H^+$ which occurred in the aqueous solution [53]. It has been determined that most of the fluoride released from model glass-ionomer cements is in complexed form rather than as "free" $F^-$ [54]. Therefore, it can be assumed that the presence of Zn in glass particles interferes with the release of $F^-$. As a result, AG glasses that release greater amounts of $Zn^{2+}$ than BioUnion filler (Cont) demonstrated less release of $F^-$ across all three pH conditions. Overall, AGs are more suitable than BioUnion filler for applications where the greater release of $Zn^{2+}$ is desired.

The result of antibacterial testing indicated that the inhibition of *S. mutans* by AGs was significantly greater with the decrease in the pH of the bacterial suspension. Further, BioUnion filler did not exhibit significant inhibition of *S. mutans* at pH 7.0 and 6.0 despite the release of $Zn^{2+}$, while AGs exhibited significant inhibition across all pH conditions. The mechanistic insights provided by this study highlight the role of Zn in enhancing antibacterial activity, as AGs released greater amounts of $Zn^{2+}$ than BioUnion filler. To determine the inhibitory effect of the components $Zn^{2+}$ and $F^{-}$, the MICs and MBCs against *S. mutans* were measured via a microdilution assay. An MBC of 4.8 mg/ml (480 ppm) for NaF against *S. mutans* has been reported [55]. Our previous study reported an MIC of 128 ppm and MBC of 2048 ppm for $F^{-}$ against *S. mutans* [56]. The MIC of NaF against *S. mutans* in this study was 125 ppm, while the MBC was over 500 ppm. All the concentrations of $F^{-}$ released from the four groups were smaller than the MIC of $F^{-}$. Therefore, the antibacterial activity of these glasses was found to be due to the release of $Zn^{2+}$. Hernández-Sierra *et al.* [57] reported an MIC range of 500 ± 306.18 μg/ml (500 ± 306.18 ppm) and MBC of 500 μg/mL (500 ppm) for ZnO-nanoparticles against *S. mutans*. Yu *et al.* [58] reported an MIC of 0.156 mg/mL (156 ppm) and MBC of 0.312 mg/mL (312 ppm) for ZnO-nanoparticles against *S. mutans*. Salts (zinc chloride, zinc gluconate) and ZnO-nanoparticles are the most common forms used in the evaluation of MICs and MBCs [59], while zinc nitrate ($Zn(NO_3)_2$) was rarely reported. In this study, the MIC of $Zn(NO_3)_2$ for *S. mutans* was 125 ppm, while the MBC was 250 ppm. The concentrations of $Zn^{2+}$ released at pH 5.0 and 6.0 from AG-1, AG-2, and AG-3 were greater than the MIC (125 ppm) against *S. mutans*, while the

concentrations of $Zn^{2+}$ released from AG-2 at pH 5.0 and AG-3 at pH 5.0 and 6.0 were greater than the MBC (250 ppm) against *S. mutans*. Liu *et al.* [45] reported that the concentration of $Zn^{2+}$ released from BioUnion filler (Cont) in acetic acid at pH 5.5 was 166.9 ± 11.2 ppm. In this study, the concentration of $Zn^{2+}$ released from AG-3 in the medium adjusted to pH 6.0 was 278.7 ± 11.0 ppm, greater than that of $Zn^{2+}$ released from BioUnion filler at pH 5.5. These quantitative results demonstrate the enhanced antibacterial activity of the new glasses, particularly under acidic conditions, and support the hypothesis that replacing Ca with Zn in the BioUnion filler improves antibacterial effectiveness. As supported by these results, AG-3 demonstrated bactericidal effects (the number of bacteria was smaller than the initial concentration of bacteria) at pH of 5.0 as well as 6.0, due to the effective release of $Zn^{2+}$.

While the pH of supragingival plaque typically ranges from approximately 6.7 to 7.3 as described above, the pH of the plaque decreases below 5.5 when acidogenic bacteria in supragingival plaque metabolize carbohydrates and produce acids [60, 61]. Nonetheless, the buffering capacity of saliva facilitates the gradual return of plaque pH to a neutral state over time. Therefore, the experiments in this study that evaluated on-demand $Zn^{2+}$-releasing properties and antibacterial effects of AG glasses involves immersing the materials in an acidic solution at pH 5.0 for 1 day to simulate the brief acidic exposure, followed by 3 days in a neutral solution at pH 7.0 to mimic neutral environments. During the experiment's period, the amounts of $Zn^{2+}$ released from AG-2 and AG-3 into acids were continuously greater than the MBC of $Zn^{2+}$ against *S. mutans*, which explained that AG-2 and AG-3 maintained killing effects against *S.*

*mutans* under the acidic condition after two-time exposures to acid. Furthermore, AG-3 exhibited the strongest bactericidal effects amongst all glasses; thereby, it was chosen to be incorporated into resins and used for the further experiments.

Several attempts have been made to incorporate Zn-containing glasses into dental resins to achieve antibacterial effects against oral bacteria through the release of $Zn^{2+}$ from the glasses. Lee *et al.* [39] incorporated Zn-doped silicate-based glass into a TEGDMA-based orthodontic adhesive. They investigated inhibitory effect against *S. mutans* by measuring the turbidity of the bacterial suspension after incubation for 24 or 48 hours in the presence of the experimental adhesive. However, it was found that there was no significant difference between the control adhesive incorporating silicate-based glass without Zn and the experimental adhesive incorporating silicate-based glass containing 5 (wt)% Zn. Lee *et al.* [62] fabricated phosphate-based glass containing 16 mol% Zn and incorporated it into a commercial flowable resin composite (G-aenial Universal Flo, GC), whose primary component in the matrix resin is urethane dimethacrylate (UDMA). In agar diffusion tests and bacterial adhesion tests, the experimental resins incorporating 3.8% and 5.4% phosphate-based Zn-containing glass produced greater inhibition zones against *S. mutans* and decreased the number of bacteria adhering to the resin composites compared with the control resin without glass. However, these approaches typically employ a simple design to exhibit the release of $Zn^{2+}$ under non-controlled manners. In this study, the acidity-responsive $Zn^{2+}$-releasing silicate-based glass (AG-3) was incorporated into dental resins to achieve antimicrobial effects through the controlled release of $Zn^{2+}$ in response to pH decrease in the dental

biofilm. Additionally, AG-3 was incorporated into dental resins and designed to dissolve in the acidic wet environment. Therefore, 10 (wt)% of the hydrophilic monomer HEMA was added to the experimental resin composition to enhance the hydrophilicity of the TEGDMA-based dimethacrylate resin. By the on-disc culture assay, the number of viable *S. mutans* on all experimental resins incorporating AG-3 at 10, 20, and 30 (wt)% decreased at pH 5.0 and 6.0 compared with pH 7.0. Furthermore, at pH 5.0 and 6.0, the experimental resin incorporating 30 (wt)% AG-3 demonstrated a significantly smaller number of viable cells compared with both the control resin and the experimental resins incorporating 10 and 20 (wt)% AG-3. This decrease was also notable when compared with the initial bacterial amount, suggesting that the experimental resin incorporating 30 (wt)% AG-3 exhibited effective bactericidal properties under acidic conditions. Therefore, the experimental resin incorporating 30 (wt)% AG-3 was selected for further evaluation.

The on-demand $Zn^{2+}$ release of experimental resin incorporating 30 (wt)% AG-3 was confirmed using the same method that examined the $Zn^{2+}$ release of AGs. The results indicated that the concentrations of $Zn^{2+}$ released from the experimental resin incorporating 30 (wt)% AG-3 increased repeatedly in response to exposure to acids. The average weight of the experimental resin disc incorporating 30 (wt)% AG-3 used in this experiment was around 35.0 mg, indicating there was 10.5 mg of AG-3 in the experimental resin. According to the 42.2 (mol)% of ZnO content in AG-3, the weight percentage of ZnO in AG-3 is 39.8%. Accordingly, there was around 3.4 mg of Zn in AG-3 incorporated in the experimental resin. Given that about 350 ppm of $Zn^{2+}$ leached

out in 200 μL of acetate buffer, around 0.07 mg of Zn was determined. Therefore, the release rate of $Zn^{2+}$ from AG-3 in the experimental resin into acetate buffer was around 2%. If all Zn incorporated in the resin were released, it would be capable of releasing $Zn^{2+}$ with 48 times exposures to acid over 144 days. Although it is not possible to precisely determine the duration of $Zn^{2+}$ release in clinical settings based on the results of this study, long-term on-demand release of $Zn^{2+}$ from dental resins incorporating AG-3 can be expected. SEM observation confirmed that particles of AG-3 remained well-integrated in the experimental resin even after repeated exposures to acid. The result suggested that the addition of AG-3 had minimal impact on the physical properties of the resin, even under acidic conditions. In the on-disc culture assay, the antibacterial effect of the dental resin incorporating AG-3 under the acidic condition remained at the same level before and after repeated exposures to acid. The result indicated that the killing effects of the dental resin incorporating 30 (wt)% AG-3 against *S. mutans* were maintained under acidic conditions, even after repeated exposures to acid. This suggests that the long-term on-demand release of $Zn^{2+}$ from the dental resin incorporating 30 (wt)% AG-3 would lead to long-lasting antimicrobial effects.

To evaluate the anti-biofilm effect of the dental resin incorporating 30 (wt)% AG-3 after repeated exposures to acetate buffer and HEPES, an *in vitro* assessment simulating oral biofilm formation process was conducted. Initially, the specimens were immersed in saliva to form an initial conditioning layer on the surface, as saliva contains proteins and other components that facilitate bacterial adhesion [63]. Following this, the 12-hour immersion in *S. mutans* suspension provided the time for bacteria to adhere

and begin forming microcolonies. Further, the experimental resin was immersed in BHI medium supplemented with sucrose three times during a 24-hour incubation to simulate three meals to produce extracellular polysaccharides that strengthen the biofilm's structural integrity [64]. The SEM and CLSM observations indicated that the dental resin incorporating 30 (wt)% AG-3 exhibited a greater percentage of membrane-compromised bacteria, which are likely dead, with a reduced biofilm thickness when compared with the control resin without AG-3. By immersion in the 2% sucrose-supplemented medium three times for total 60 minutes, the pH of biofilm formed on specimens would be decreased by the acid production from *S. mutans*. This condition might be preferable for the experimental resin incorporating AG-3 that can release $Zn^{2+}$ under acidic conditions and kill the bacteria in *S. mutans* biofilm. However, oral microbes consist of diverse microorganisms that produce more complex and harsher biofilms. Therefore, an assessment of the benefits of experimental resin by using multispecies biofilm is required to determine its potential for clinical applications in the future.

Despite the antibacterial property of dental resin incorporating AG-3 was proven by this study, the experiments were primarily conducted under laboratory conditions, lacking evaluation of long-term effects in clinical applications. Therefore, future research should focus on validating the antibacterial performance and stability *in situ*. Besides, this study did not thoroughly explore the potential impact of incorporating AG-3 into resins on physical properties, such as strength, wear resistance, and bond strength. Future research needs to comprehensively assess the effects of composition

optimization on these performance metrics to ensure clinical feasibility. In addition, the current study focused on the antibacterial property of the resin without considering the issue of bacterial resistance development. With the widespread use of antibacterial materials, bacteria may develop resistance; thus, future research should address the impact of the novel material on bacterial resistance and explore potential solutions. Moreover, future research should systematically explore the effects of different compositions and process parameters on the antibacterial properties and physical characteristics of resin composition to determine the specific approach, such as coating resins, restorative resins, or adhesive resins.

## 1.4 Summary

The acidity-responsive $Zn^{2+}$-releasing glass was successfully fabricated, which effectively released $Zn^{2+}$ under acidic conditions, achieving exhibition of on-demand killing effects against bacteria in the dental plaque when incorporated into dental resins.

# EXPERIMENT 2

# Fabrication of rapidly soluble $Zn^{2+}$-releasing glass and incorporation into dental resin

## 2.1 Materials and methods

### 2.1.1 Fabrication of rapidly soluble $Zn^{2+}$-releasing glass (RG)

The rapidly soluble phosphate-based glass containing Zn (RG) was fabricated by the melt-quenching method. Briefly, phosphoric acid ($H_3PO_4$), sodium carbonate ($Na_2CO_3$), calcium carbonate ($CaCO_3$), and zinc oxide (ZnO), purchased from FUJIFILM Wako Pure Chemical Corporation, were mixed and melted in the furnace at 1100℃ for 1 hour. The melted glass was quenched at room temperature and pressed by an iron plate to obtain a glass cullet. The glass cullet was ground to particles with ethyl alcohol by a rotating ball mill machine (Pot Mill Rotary Stand, Nitto Kagaku, Nagoya, Japan). The ground particles were passed through a stainless-steel sieve (250-μm mesh testing sieve, Nonaka Rikaki) to exclude the particles that were not sufficiently ground. The mixing ratio of the components was 42.0 $P_2O_5$, 40.0 $Na_2O$, 4.0 CaO, and 12.0 ZnO in the mol fraction. The glass particles were sterilized with ethylene oxide gas.

### 2.1.2 Characterization of RG

High-resolution imaging of the RG surface and its elemental mapping was obtained by field emission scanning electron microscopy (FE-SEM; JSM-F100, JEOL) and energy

dispersive spectroscopy (EDS; JSM-F100, JEOL). The glass structure was confirmed by an X-ray diffraction detector (XRD; PIXcel$^{1D}$, Malvern Panalytical Ltd.). The size distribution of glass particles was measured by a particle size analyzer (Partica LA-960V2, Horiba). The elemental composition of each glass was analyzed by X-ray fluorescence (XRF; ZSX Primus IV$i$, Rigaku).

### 2.1.3 Evaluation of solubility and ion-releasing property of RG

The solubility of RG in the buffer solution with different pH values was evaluated. The buffer solution was prepared by 4-(2-hydroxyethyl)-1-piperazineethanesulfonic acid (HEPES; FUJIFILM Wako Pure Chemical) at pH 7.0 and acetate buffer (Kanto Chemical) at pH 6.0 or 5.0. Fifty mg of RG was immersed in 10 mL of each buffer solution. After 100-rpm gyratory shaking at 37°C for 24 hours, the suspensions were filtered through a 55 mm glass fiber filter with a pore size of 0.5 μm (ADVANTEC) which was weighed beforehand. The glass fiber filter was dried at 110°C for 6 hours. The total weight of the undissolved glass and the glass fiber filter was measured, and the solubility of RG was calculated. The experiment was repeated five times.

The concentration of $Zn^{2+}$ released from RG into pH-adjusted BHI broth was evaluated. The pH of BHI broth was adjusted by adding hydrochloride acid (HCl; Kanto Chemical) until reaching the value of 7.0, 6.0, or 5.0. Twenty mg of RG was placed in a well of a 96-well microplate, and 200 μL of pH-adjusted BHI broth was poured into the wells containing glass particles. After 100-rpm gyratory shaking at 37°C for 24 hours, the suspensions were passed through a 0.22 μm syringe filter (Merck Millipore

Ltd.) and diluted with 9.8 mL distilled water. The dilutions were used for determining the concentration of $Zn^{2+}$ with an inductively coupled plasma-optical emission spectrometer (ICP-OES; iCAP7200 ICP-OES Duo, Thermo Fisher Scientific). The experiment was repeated five times.

### 2.1.4 Bacteria used

*Lactobacillus casei* ATCC4646, *Actinomyces naeslundii* ATCC19246, *Enterococcus faecalis* SS497, *Fusobacterium nucleatum* 1436, and *Parvimonas micra* GIFU7745, were selected as ones detected in the deep caries (Table 4). *Streptococcus mutans* NCTC10449 was used as a reference.

Before being used in the following experiments, each bacterium was anaerobically cultured from a stock culture at 37°C using the medium described in Table 4. *E. faecalis* was cultured for 12 hours, *A. naeslundii* was cultured for 48 hours, *L. casei*, *F. nucleatum*, *P. micra*, and *S. mutans* were cultured for 24 hours.

### 2.1.5 Measurements of MICs and MBCs of $Zn^{2+}$ against oral bacteria

The values of MICs and MBCs of $Zn^{2+}$ against *L. casei, A. naeslundii, E. faecalis, F. nucleatum* and *P. micra* were measured with the broth dilution method. The Zn standard solutions were obtained by dissolving zinc nitrate hexahydrate ($Zn(NO_3)_2 \cdot 6H_2O$; Kanto Chemical) into distilled water. Fifty μL of standard solutions with a concentration of 32.5 – 32000 ppm obtained after serial two-fold dilutions were poured into the wells of a 96-well microplate. Fifty μL of each bacterial suspension, adjusted to

approximately $2.0 \times 10^6$ CFU/mL in double-concentration broth, was poured into each well containing the standard solutions to prepare 16.25 – 16000 ppm of Zn solutions with $1 \times 10^6$ CFU/mL of bacterial suspension. After anaerobic incubation at 37°C for 24 hours, the turbidity of the suspensions was observed visually, and the MIC, which is the lowest concentration that prevents visible bacterial growth, was determined. Twenty of the samples with no visible turbidity were inoculated on agar plates. After anaerobic incubation at 37°C for 48 hours, the MBC, which is the lowest concentration of the agent that kills the bacterium, was determined using the agar plates with no bacterial colonies. The experiment was repeated five times.

### 2.1.6 Evaluation of antibacterial activity of RG against oral bacteria

The antibacterial activity of RG against *L. casei, A. naeslundii, E. faecalis, F. nucleatum, P. micra* and *S. mutans* was evaluated. Each bacterial suspension was adjusted to approximately $1 \times 10^6$ CFU/mL in respective broth listed in Table 4. A total of 20 mg of RG was placed in a well of a 96-well microplate, and 200 μL of each bacterial suspension was poured into the wells containing glass particles. After anaerobic incubation at 37°C for 24 hours, 100 μL of each bacterial suspension was collected and diluted with 9.9 mL of respective broth. The suspensions were serially diluted with respective broth and 100 μL of dilutions were inoculated on respective agar plates listed in Table 4. After anaerobic incubation at 37°C for 48 hours, the number of colonies on the agar plates was counted. The bacterial suspensions incubated in the absence of RG were used as control groups. The experiment was repeated five times.

### 2.1.7 Fabrication of dental resin incorporating RG

The experimental resin was prepared by mixing RG with TEGDMA, HEMA, CQ, EPA, and BHT (Table 2). The particles of RG and the liquid of uncured resin were mixed in a ratio of 1:9 (w/w), providing 10 (wt)% RG in the experimental resin. The resin without RG was used as a control.

### 2.1.8 Evaluation of inhibition of bacteria in dentinal tubules by dental resin incorporating RG

To evaluate the inhibitory effect of dental resin incorporating RG against bacteria in dentinal tubules, the infected dentin models were prepared according to the method reported by Kitagawa *et al*. [65] (Figure 22). Extracted human sound molars were obtained from patients at Osaka University Dental Hospital under a protocol approved by the Ethics Review Committee of Osaka University Graduate School of Dentistry and Osaka University Dental Hospital (Approval number: R1-E52). The teeth were cut with a low-speed diamond saw (Isomet 2000, Buehler, Lake Bluff, IL, USA) under water cooling, and rectangular parallelepiped specimens were obtained from the coronal dentin about 1 mm above the coronal pulp. The dimension of the specimens was adjusted using a grinder (EcoMet 3000, Buehler) to 4 mm in length, 2 mm in width, and 2 mm in height.

To remove the smear layer and open the dentinal tubules, the dentin specimens were immersed sequentially in 5.25% sodium hypochlorite (NaClO; Neo Dental Chemical Products CO., Tokyo, Japan) and 18% ethylenediaminetetraacetic acid

(EDTA; Ultradent Products, South Jordan, UT, USA) for 10 minutes with ultrasonication at 37 kHz. The specimens were autoclaved at 120°C for 20 minutes and anaerobically incubated in BHI broth at 37°C for 48 hours to confirm sterilization. The bottom and side surfaces of specimens were covered with double layers of nail varnish.

The suspensions of *L. casei* and *S. mutans* were adjusted to approximately $1 \times 10^6$ CFU/mL. The specimens were anaerobically incubated in 5 mL of each bacterial suspension at 37°C, while the culture medium was exchanged every 24 hours. After 7 days, the inoculated dentin specimens were rinsed in distilled water for 5 seconds. The specimens were divided into two groups: one group kept moist, while the surface of the other group was dried by air-blow for 5 seconds. The resin incorporating 10 (wt)% RG was applied on the top surface of the dentin specimens with a sterile micro brush (Microbrush Fine, Shofu, Kyoto, Japan) and left for 30 seconds, followed by 10-second light-curing (Pencure 2000, Morita) with the light intensity of 2,000 mW/cm$^2$. The dentin specimens were rinsed with distilled water and divided into two pieces by hand. The surface of the cross-section was stained with LIVE/DEAD$^{TM}$ BacLight$^{TM}$ Bacterial Viability Kit (L-7007, Thermo Fisher Scientific) according to the manufacturer's instructions. Briefly, 2 μL of component A (SYTO 9 dye, 1.67 mM/ propidium iodide, 1.67 mM solution in DMSO) and 2 μL of component B (SYTO 9 dye, 1.67 mM/ propidium iodide, 18.3 mM solution in DMSO) were mixed in 1 mL of distilled water. A hundred μL of the mixed solution was dropped on the specimens and incubated at 37°C for 15 minutes under the dark condition. After gently irrigating with distilled water, the specimens were visualized by confocal laser scanning microscopy (CLSM;

LSM 700, Carl Zeiss) at 488 and 555 nm for excitation, and 500 and 635 nm for emission. The images were obtained using a ZEN Imaging Software (Carl Zeiss). A preliminary image was taken to determine the acquisition parameters and the setting was kept constantly for all images. Scans were taken in 12 bits at a resolution of 1024 by 1024 with the following setting: Speed = 8; Pinhole size = 34 μm; Digital offset = 0; Master gain (Ch1, SYTO 9) = 493; Master gain (Ch2, propidium iodide) = 706. Three images were obtained from one sample, and the images were analyzed by Imaris software (Bitplane). The resin without RG was used as a control, and the experiment was repeated three times.

### 2.1.9 Statistical analysis

Statistical analyses were performed using SPSS Statistics 25 (IBM). The homogeneity of variances was confirmed initially. The results of solubility and ion release were statistically analyzed by the analysis of variance (ANOVA) and Tukey's honestly significant difference (HSD) test. $p < 0.05$ was considered to indicate significance in this study. The bacterial growth was analyzed by student's *t*-test with a significance level of $p < 0.05$.

## 2.2 Results

### 2.2.1 Characteristics of RG

The FE-SEM images of the experimental RG particles revealed that the glass was in

irregular shapes (Figure 23 (A)). The EDS mapping images confirmed that P, Na, Ca, Zn dispersed in the particles homogeneously (Figure 23 (B)). The size distribution of RG particle is shown in Figure 24 (A), and the median diameter of the glass particles was approximately 11.95 μm. The sample structure was amorphous, which was revealed by the XRD patterns (Figure 24 (B)). As obtained from XRF analysis, $P_2O_5$, $Na_2O$, CaO, and ZnO were detected in RG at 41.2, 40.4, 4.5, and 11.9 mol%, respectively. No remarkable difference in composition was observed between the preparation and result of the XRF analysis.

### 2.2.2 Solubility and ion-releasing property of RG

Figure 25 shows the solubility of RG particles in the pH-adjusted buffer solution (pH 7.0, 6.0, or 5.0). The dissolution rate at pH 7.0, 6.0, and 5.0 was 98.7 ± 0.31%, 96.4 ± 0.63%, and 93.8 ± 0.92%, respectively. Across all three pH conditions, the solubility of RG after 24 hours was over 90%.

The concentration of $Zn^{2+}$ released from RG into the pH-adjusted BHI broth (pH 7.0, 6.0, or 5.0) is shown in Figure 26. The concentration of $Zn^{2+}$ released from RG at pH 7.0, 6.0, and 5.0 was 8172.5 ± 299.8 ppm, 6851.6 ± 98.2 ppm, and 5978.5 ± 63.7 ppm, respectively. Across all three pH conditions, the concentrations of released $Zn^{2+}$ were beyond 5900 ppm.

### 2.2.3 MICs and MBCs of $Zn^{2+}$ against oral bacteria

The MICs and MBCs of $Zn^{2+}$ against *L. casei*, *A. naeslundii*, *E. faecalis*, *P. micra*, and

*F. nucleatum* are shown in Table 5. For the five species, the MIC values ranged from 62.5 to 1000 ppm and the MBC values ranged from 125 to 4000 ppm.

### 2.2.4 Antibacterial activity of RG against oral bacteria

Figure 27 shows the number of each viable bacteria after incubation in the presence of RG particles. The number of surviving cells of all bacterial species significantly decreased after incubation with RG particles. Although RG particles demonstrated only a 3 – 4 log reduction in bactericidal effect against *E. faecalis*, they showed a 100% killing effect against all other bacteria.

### 2.2.5 Inhibition of bacteria in dentinal tubules by dental resin incorporating RG

CLSM analysis confirmed that the depth of *L. casei* penetration in the dentinal tubules reached approximately 148 ± 80 μm (Figure 28 (A)). When the dentin specimens were dried, some viable bacteria remained in the dentinal tubules after treatment with experimental resin incorporating RG (Figures 28 (B). In contrast, in the wet state, the dental resin incorporating RG completely eradicated *L. casei* in the dentinal tubules (Figures 28 (C)), while the control resin without RG did not exhibit antimicrobial effects against *L. casei* in dentinal tubules (Figure 28 (D)).

The depth of *S. mutans* penetration in the dentinal tubules was approximately 212 ± 71 μm (Figure 29 (A)). When the dentin specimens were dried, some viable *S. mutans* remained in the dentinal tubules after treatment with experimental resin incorporating RG (Figure 29 (B)). Under the wet condition, the dental resin incorporating RG

completely eradicated *S. mutans* in the dentinal tubules (Figure 29 (C)). The control resin without RG did not exhibit antimicrobial effects against *S. mutans* in dentinal tubules (Figure 29 (D)).

## 2.3 Discussion

Phosphate-based glass is a promising new-generation biomaterial with excellent biocompatibility and versality, which allow researchers to design biomaterials with properties optimized for various medical applications [18]. The bridging P-O-P bonds in the glass network structure are easily hydrolyzed in aqueous media due to high susceptibility to proton attack [11]. The addition of cations such as $Zn^{2+}$ is helpful to aid glass formation and strengthen the glass network by suppressing glass crystallization and extending the glass-forming region of polyphosphate glass [66]. In addition, ZnO improves the chemical stability of phosphate glass by forming [$ZnO_4$] tetrahedral or P-O-Zn bridges in the glass network structure [67]. Previous studies claimed that the pyrophosphates ($P_2O_7^{4-}$) were present in the structure of phosphate-based glasses when the content of $P_2O_5$ in the glass was less than 50 mol% [68]. Pyare *et al.* [69] observed the increased solubility of phosphate glasses with 50% mol of $P_2O_5$ with increasing pH and suggested the hydroxyl ions ($OH^-$) break the P-O-P bonds through the hydrolysis reaction: $P_2O_7^{4-} + OH^- \rightarrow 2HPO_4^{2-}$. Even in the presence of glass network modifier such as ZnO, the Zn-O-P linkage is easily attacked by $OH^-$ through the reaction: Zn-O-P + $OH^- \rightarrow Zn(OH)_2 + HPO_4^{2-}$. In this study, the mol fraction of

$P_2O_5$ in RG was 41.2 mol%, which suggested the glass structure of $P_2O_7^{4-}$, and thus resulting in its reduced solubility and $Zn^{2+}$ release with decreasing pH. Nevertheless, the solubilities of RG after 24 hours were over 90% and the concentrations of released $Zn^{2+}$ were beyond 5900 ppm across all three different pH conditions, indicating its ability to release high concentration of $Zn^{2+}$ in a short period.

According to many reports regarding the microbiome associated with the deep caries, *Lactobacillus spp.*, *Actinomyces spp.*, *Fusobacterium spp., and Streptococcus spp.*, are prevalent in the deep carious lesions [70-73]. It has been also shown that *P. micra* was detected in carious dentin [74] and irreversible pulpitis [75, 76]. *E. faecalis* is isolated from deep caries legions and infected root canals [77, 78]. In this study, the MIC values of $Zn^{2+}$ against *L. casei, A. naeslundii, F. nucleatum, P. micra* and *E. faecalis* were 500, 62.5, 125, 125, and 1000 ppm, respectively, and the MBC values were 2000, 125, 500, 250, and 4000 ppm, respectively. Over 5900 ppm of $Zn^{2+}$, which was significantly greater than the MIC and MBC values against each tested bacteria, was released from RG particles under three pH conditions (pH 5.0, 6.0, and 7.0). Therefore, the amount of $Zn^{2+}$ released from RG particles was sufficient to exhibit a bactericidal effect on the bacterial species. However, RG particles demonstrated only a 3 – 4 log reduction in bactericidal effect against *E. faecalis*, whereas they showed a 100% killing effect against all other bacteria. Unlike other bacterial species tested in this study, *E. faecalis* are natural members of the intestinal flora and therefore able to survive in a wide range of pH, heating and high metal concentrations [79]. Zincophore biosynthetic gene clusters are identified in a broad range of bacteria, including

actinobacteria, clostridia, fusobacteria, and bacilli, suggesting potential targets for antimicrobial therapies [80]. Likewise, Zn-responsive proteins were also detected in *E. faecalis* genes, which are responsible for mediating bacterial defense against zinc overload [81] and suggested the reason why *E. faecalis* was less affected by $Zn^{2+}$ released from RG particles compared with other bacteria. Due to the ability to survive and persist as a pathogen in the dentinal tubules, many studies have been devoted to find an effective way to eradicate *E. faecalis*, and the antimicrobial activity against *E. faecalis* of Zn-containing sealers has been proved [82].

The level of bacterial infection after caries removal varies clinically. Hirose *et al.* [83] established dentin models with different infection levels by culturing the dentin specimens in *S. mutans* suspension for 6 or 12 hours. Both models showed bacterial penetration into the dentinal tubules up to approximately 50 μm from the surface. Kitagawa *et al.* [65] prepared infected dentin specimens by immersing the root dentin in *E. faecalis* suspension for 2 days, resulting in *E. faecalis* penetrating approximately 200 μm into the dentinal tubules. In this study, a dentin model infected with *L. casei*, which was one of the most prevalent species in deep caries lesions, was first established by culturing the dentin specimens in the *L. casei* suspension. Preliminary experiments indicated no clear bacterial penetration into the dentinal tubules after incubating dentin specimens in *L. casei* suspension for 2 days. Therefore, dentin specimens were immersed in *L. casei* suspension for 7 days in this study, resulting in *L. casei* penetrating approximately 150 μm into the dentinal tubules. The dentin specimens immersed in *S. mutans* suspension for 7 days showed bacterial penetration up to about 200 μm, but

there was no significant difference in the penetration depth between *L. casei* and *S. mutans*. Factors influencing bacterial penetration include the dentinal tubules status (size and orientation), microorganism size, and bacterial motility [84, 85]. *L. casei* is nonmotile, rod-shaped with the size of 0.7 – 1.1 μm × 2.0 – 4.0 μm and often exists singly or in short chains [86]. Its rod shape allows it to enter dentinal tubules, but its motility is relatively limited compared to other bacteria. *S. mutans* are spherical (0.5 – 0.75 μm in diameter) in pairs or chains [87]. Both bacteria are small enough to enter dentinal tubules (3.47 ± 0.73 μm for permanent teeth) [88], and their penetration is likely driven by diffusion and passive processes rather than active movement [89]. The acid production by both bacteria can demineralize dentin, potentially enlarging the tubules and aiding deeper penetration. The similarity in penetration depth suggested that factors other than morphology, such as acid production and the intrinsic properties of dentin, played a more crucial role in determining how far these bacteria can infiltrate the dentinal tubules. Overall, the usage of *S. mutans* as a reference to *L. casei* is important, indicating the validity of the infection model to evaluate the inhibition of bacteria in dentinal tubules by dental resin incorporating RG.

Using these established infected dentin models, the antibacterial effect of the experimental resin was examined. It was found that under a wet condition, compared with a dry state, the bacteria in the dentin were effectively killed. The result indicated the difference of $Zn^{2+}$ release between wet and dry condition due to the dissolution of glass in the experimental resin. Designed as cavity liner or pulp-capping material, the experimental resin incorporating RG dissolves in a sealed cavity, which is typically

associated with wet or moist conditions. In that case, $Zn^{2+}$ would be released soon and penetrate deeply into the dentinal tubules, resulting in rapidly killing bacteria.

The infected dentin model established in this study did not fully replicate the complex environment of the dentinal cavity including multiple bacterial species. *In vivo* studies are crucial to evaluate clinical effectiveness of the experimental resin incorporating RG, while also optimizing the composition of the resins. In addition, it is essential to investigate whether the rapid solubility of the glass could lead to adverse effects, such as weakening of the resin structure or negative reactions in the surrounding tissues over time.

## 2.4 Summary

The rapidly soluble $Zn^{2+}$-releasing glass was successfully fabricated, which released high concentration of $Zn^{2+}$ in a short period under the wet condition regardless of pH, being useful for killing bacteria in dentinal tubules when incorporated into dental resin.

# GENERAL CONCLUSION

Glass containing Zn holds great potential in the dental field, particularly due to its broad-spectrum antibacterial activity, biocompatibility, and enhanced mechanical properties. However, the controlled release of $Zn^{2+}$ still poses challenge to the clinical applications. With the objective to develop novel antimicrobial materials in response to various usage conditions, acidity-responsive $Zn^{2+}$-releasing glass and rapidly soluble $Zn^{2+}$-releasing glass were fabricated.

The acidity-responsive $Zn^{2+}$-releasing glass (AG) demonstrated increased $Zn^{2}$ release and effective antibacterial ability under acidic conditions. The AG-3 glass with 42.7 (mol)% Zn was selected to be incorporated into dental resins based on its extensive properties. By incorporating 30 (wt)% AG-3, the dental material is believed to exhibit antibacterial effects on demand in response to acidity.

The rapidly soluble $Zn^{2+}$-releasing glass (RG) demonstrated increased solubility and $Zn^{2+}$-releasing property under neutral pH conditions. In addition to its bactericidal effects against oral bacteria, the dental resin incorporating 10 (wt)% RG demonstrated killing effects against bacteria in dentinal tubules.

Overall, the two novel glasses developed in this study enabled the controlled release of $Zn^{2+}$, allowing for conferring possible clinically effective antibacterial activities to dental materials under their usage conditions.

# REFERENCES

[1] Weintraub JA. The *Oral Health in America* report: a public health research perspective. Preventing Chronic Disease. 2022; 19: E58.

[2] Gendron R, Grenier D, Maheu-Robert LF. The oral cavity as a reservoir of bacterial pathogens for focal infections. Microbes and Infection. 2000; 2: 897-906.

[3] Boyd D, Li H, Tanner D, Towler MR, Wall J. The antibacterial effects of zinc ion migration from zinc-based glass polyalkenoate cements. Journal of Materials Science: Materials in Medicine. 2006; 17: 489-494.

[4] Esteban-Tejeda L, Prado C, Cabal B, Sanz J, Torrecillas R, Moya JS. Antibacterial and antifungal activity of ZnO containing glasses. PLOS ONE. 2015; 10: e0132709.

[5] Raja FNS, Worthington T, Isaacs MA, Rana KS, Martin RA. The antimicrobial efficacy of zinc doped phosphate-based glass for treating catheter associated urinary tract infections. Materials Science and Engineering: C. 2019; 103: 109868.

[6] Cummins D. Zinc citrate/triclosan: a new anti-plaque system for the control of plaque and the prevention of gingivitis: short-term clinical and mode of action studies. Journal of Clinical Periodontology. 1991; 18: 455-461.

[7] He G, Pearce EIF, Sissons CH. Inhibitory effect of $ZnCl_2$ on glycolysis in human oral microbes. Archives of Oral Biology. 2002; 47: 117-129.

[8] Sheng J, Nguyen PTM, Marquis RE. Multi-target antimicrobial actions of zinc against oral anaerobes. Archives of Oral Biology. 2005; 50: 747-757.

[9] Phan TN, Buckner T, Sheng J, Baldeck JD, Marquis RE. Physiologic actions of zinc related to inhibition of acid and alkali production by oral streptococci in suspensions and biofilms. Oral Microbiology and Immunology. 2004; 19: 31-38.

[10] Koo H, Sheng J, Nguyen PT, Marquis RE. Co-operative inhibition by fluoride and zinc of glucosyl transferase production and polysaccharide synthesis by mutans streptococci in suspension cultures and biofilms. FEMS Microbiology Letters. 2006; 254: 134-140.

[11] Bunker BC, Arnold GW, Wilder JA. Phosphate glass dissolution in aqueous solutions. Journal of Non-Crystalline Solids. 1984; 64: 291-316.

[12] Devreux F, Barboux P, Filoche M, Sapoval B. A simplified model for glass dissolution in water. Journal of Materials Science. 2001; 36: 1331-1341.

[13] Cailleteau C, Weigel C, Ledieu A, Barboux P, Devreux F. On the effect of glass

composition in the dissolution of glasses by water. Journal of Non-Crystalline Solids. 2008; 354: 117-123.

[14] Chen X, Brauer DS, Karpukhina N, Waite RD, Barry M, McKay IJ, Hill RG. 'Smart' acid-degradable zinc-releasing silicate glasses. Materials Letters. 2014; 126: 278-280.

[15] Struzycka I. The oral microbiome in dental caries. Polish Journal of Microbiology. 2014; 63: 127-135.

[16] Lamont RJ, Koo H, Hajishengallis G. The oral microbiota: dynamic communities and host interactions. Nature Reviews Microbiology. 2018; 16: 745-759.

[17] Radaic A, Kapila YL. The oralome and its dysbiosis: new insights into oral microbiome-host interactions. Computational and Structural Biotechnology Journal. 2021; 19: 1335-1360.

[18] Knowles JC. Phosphate based glasses for biomedical applications. Journal of Materials Chemistry. 2003; 13: 2395-2401.

[19] Pitts NB, Ekstrand KR. International Caries Detection and Assessment System (ICDAS) and its International Caries Classification and Management System

(ICCMS) - methods for staging of the caries process and enabling dentists to manage caries. Community Dentistry and Oral Epidemiology. 2013; 41: e41-52.

[20] Maltz M, Henz SL, de Oliveira EF, Jardim JJ. Conventional caries removal and sealed caries in permanent teeth: a microbiological evaluation. Journal of Dentistry. 2012; 40: 776-782.

[21] Lim ZE, Duncan HF, Moorthy A, McReynolds D. Minimally invasive selective caries removal: a clinical guide. British Dental Journal. 2023; 234: 233-240.

[22] Schwendicke F, Tu YK, Hsu LY, Göstemeyer G. Antibacterial effects of cavity lining: a systematic review and network meta-analysis. Journal of Dentistry. 2015; 43: 1298-1307.

[23] Kunert M, Lukomska-Szymanska M. Bio-inductive materials in direct and indirect pulp capping—a review article. Materials. 2020; 13: 1204.

[24] Forsten L, Söderling E. The alkaline and antibacterial effect of seven $Ca(OH)_2$ liners *in vitro*. Acta Odontologica Scandinavica. 1984; 42: 93-98.

[25] Lado EA, Pappas J, Tyler K, Stanley HR, Walker C. *In vitro* antimicrobial activity of six pulp-capping agents. Oral Surgery, Oral Medicine, Oral Pathology. 1986; 61:

197-200.

[26] Portenier I, Haapasalo H, Rye A, Waltimo T, Ørstavik D, Haapasalo M. Inactivation of root canal medicaments by dentine, hydroxylapatite and bovine serum albumin. International Endodontic Journal. 2001; 34: 184-188.

[27] Mohammadi Z, Dummer PM. Properties and applications of calcium hydroxide in endodontics and dental traumatology. International Endodontic Journal. 2011; 44: 697-730.

[28] Kaur G, Pandey OP, Singh K, Homa D, Scott B, Pickrell G. A review of bioactive glasses: their structure, properties, fabrication and apatite formation. Journal of Biomedical Materials Research Part A. 2014; 102: 254-274.

[29] Stalons DR, Thornsberry C. Broth-dilution method for determining the antibiotic susceptibility of anaerobic bacteria. Antimicrobial Agents and Chemotherapy. 1975; 7: 15-21.

[30] Bellantone M, Coleman NJ, Hench LL. Bacteriostatic action of a novel four-component bioactive glass. Journal of Biomedical Materials Research. 2000; 51: 484-490.

[31] Blaker J, Nazhat S, Boccaccini A. Development and characterisation of silver-doped bioactive glass-coated sutures for tissue engineering and wound healing applications. Biomaterials. 2004; 25: 1319-1329.

[32] Wu C, Zhou Y, Xu M, Han P, Chen L, Chang J, Xiao Y. Copper-containing mesoporous bioactive glass scaffolds with multifunctional properties of angiogenesis capacity, osteostimulation and antibacterial activity. Biomaterials. 2013; 34: 422-433.

[33] Li J, Zhai D, Lv F, Yu Q, Ma H, Yin J, Yi Z, Liu M, Chang J, Wu C. Preparation of copper-containing bioactive glass/eggshell membrane nanocomposites for improving angiogenesis, antibacterial activity and wound healing. Acta Biomaterialia. 2016; 36: 254-266.

[34] Jung WK, Koo HC, Kim KW, Shin S, Kim SH, Park YH. Antibacterial activity and mechanism of action of the silver ion in *Staphylococcus aureus* and *Escherichia coli*. Applied and Environmental Microbiology. 2008; 74: 2171-2178.

[35] Khan K, Javed S. Functionalization of inorganic nanoparticles to augment antimicrobial efficiency: a critical analysis. Current Pharmaceutical Biotechnology. 2018; 19: 523-536.

[36] Shetty S, Sekar P, Shetty RM, Abou Neel EA. Antibacterial and antibiofilm efficacy of copper-doped phosphate glass on pathogenic bacteria. Molecules. 2023; 28: 3179.

[37] Moazami F, Sahebi S, Ahzan S. Tooth discoloration induced by imidazolium based silver nanoparticles as an intracanal irrigant. Journal of Dentistry. 2018; 19: 280-286.

[38] Cheat LW, Sing LS, editors. Copper discoloration: correlation between copper oxidation states and their colors. 2018 IEEE International Symposium on the Physical and Failure Analysis of Integrated Circuits (IPFA). 2018; 1-3.

[39] Lee SM, Kim IR, Park BS, Lee DJ, Ko CC, Son WS, Kim YI. Remineralization property of an orthodontic primer containing a bioactive glass with silver and zinc. Materials. 2017; 10: 1253.

[40] Boyd D, Li H, Tanner DA, Towler MR, Wall JG. The antibacterial effects of zinc ion migration from zinc-based glass polyalkenoate cements. Journal of Materials Science: Materials in Medicine. 2006; 17: 489-494.

[41] Clarkin O, Wren A, Thornton R, Cooney J, Towler M. Antibacterial analysis of a zinc-based glass polyalkenoate cement. Journal of Biomaterial Applications. 2011;

26: 277-292.

[42] Stefanidou M, Maravelias C, Dona A, Spiliopoulou C. Zinc: a multipurpose trace element. Archives of Toxicology. 2006; 80: 1-9.

[43] Yamamoto A, Honma R, Sumita M. Cytotoxicity evaluation of 43 metal salts using murine fibroblasts and osteoblastic cells. Journal of Biomedical Materials Research. 1998; 39: 331-340.

[44] Imazato S, Kohno T, Tsuboi R, Thongthai P, Xu HH, Kitagawa H. Cutting-edge filler technologies to release bio-active components for restorative and preventive dentistry. Dental Materials Journal. 2020; 39: 69-79.

[45] Liu Y, Kohno T, Tsuboi R, Kitagawa H, Imazato S. Acidity-induced release of zinc ion from BioUnion$^{TM}$ filler and its inhibitory effects against *Streptococcus mutans*. Dental Materials Journal. 2020; 39: 547-553.

[46] Baliga S, Muglikar S, Kale R. Salivary pH: a diagnostic biomarker. Journal of Indian Society Periodontology. 2013; 17: 461-465.

[47] Dawes C. What is the critical pH and why does a tooth dissolve in acid? Journal of the Canadian Dental Association. 2003; 69: 722-724.

[48] Heijnsbroek M, Paraskevas S, Van der Weijden GA. Fluoride interventions for root caries: a review. Oral Health and Preventive Dentistry. 2007; 5: 145-152.

[49] Kaneshiro AV, Imazato S, Ebisu S, Tanaka S, Tanaka Y, Sano H. Effects of a self-etching resin coating system to prevent demineralization of root surfaces. Dental Materials. 2008; 24: 1420-1427.

[50] Dietzel A. Strukturchemie des glases. In: Süffert F, editors. Die Naturwissenschaften. Springer, Berlin, Heidelberg; 1941; 29: 537-547.

[51] Blochberger M, Hupa L, Brauer DS. Influence of zinc and magnesium substitution on ion release from Bioglass 45S5 at physiological and acidic pH. Biomedical Glasses. 2015; 1: 93-107.

[52] Chen X, Brauer D, Karpukhina N, Waite R, Barry M, McKay I, Hill R. 'Smart' acid-degradable zinc-releasing silicate glasses. Materials Letters. 2014; 126: 278-280.

[53] Connick RE, Paul AD. The fluoride complexes of zinc, copper and lead ions in aqueous solution. Journal of the American Chemical Society. 1958; 80: 2069-2071.

[54] Billington R, Hadley P, Williams J, Pearson G. Kinetics of fluoride release from

zinc oxide-based cements. Biomaterials. 2001; 22: 2507-2513.

[55] Pradiptama Y, Purwanta M, Notopuro H. Antibacterial effects of fluoride in *Streptococcus mutans* growth *in vitro*. Biomolecular and Health Science Journal. 2019; 2: 1-3.

[56] Liu Y, Kohno T, Tsuboi R, Thongthai P, Fan D, Sakai H, Kitagawa H, Imazato S. Antibacterial effects and physical properties of a glass ionomer cement containing BioUnion filler with acidity-induced ability to release zinc ion. Dental Materials Journal. 2021; 40: 1418-1427.

[57] Hernández-Sierra JF, Ruiz F, Pena DCC, Martínez-Gutiérrez F, Martínez AE, Guillén AdJP, Tapia-Pérez H, Castañón GM. The antimicrobial sensitivity of *Streptococcus mutans* to nanoparticles of silver, zinc oxide, and gold. Nanomedicine: Nanotechnology, Biology and Medicine. 2008; 4: 237-240.

[58] Yu J, Zhang W, Li Y, Wang G, Yang L, Jin J, Chen Q, Huang M. Synthesis, characterization, antimicrobial activity and mechanism of a novel hydroxyapatite whisker/nano zinc oxide biomaterial. Biomedical Materials. 2014; 10: 015001.

[59] Almoudi MM, Hussein AS, Hassan MIA, Zain NM. A systematic review on antibacterial activity of zinc against *Streptococcus mutans*. The Saudi Dental

Journal. 2018; 30: 283-291.

[60] Schlafer S, Ibsen CJ, Birkedal H, Nyvad B. Calcium-phosphate-osteopontin particles reduce biofilm formation and pH drops in *in situ* grown dental biofilms. Caries Research. 2017; 51: 26-33.

[61] Kristensen MF, Lund MB, Schramm A, Lau EF, Schlafer S. Determinants of microscale pH in *in situ*-grown dental biofilms. Journal of Dental Research. 2023; 102: 1348-1355.

[62] Lee MJ, Seo YB, Seo JY, Ryu JH, Ahn HJ, Kim KM, Kwon JS, Choi SH. Development of a bioactive flowable resin composite containing a zinc-doped phosphate-based glass. Nanomaterials. 2020; 10: 2311.

[63] Marsh PD, Do T, Beighton D, Devine DA. Influence of saliva on the oral microbiota. Periodontology 2000. 2016; 70: 80-92.

[64] Dewar MD, Walker GJ. Metabolism of the polysaccharides of human dental plaque: I. Dextranase activity of streptococci, and the extracellular polysaccharides synthesized from sucrose. Caries Research. 1975; 9: 21-35.

[65] Kitagawa H, Kitagawa R, Tsuboi R, Hirose N, Thongthai P, Sakai H, Ueda M, Ono

S, Sasaki JI, Ooya T, Imazato S. Development of endodontic sealers containing antimicrobial-loaded polymer particles with long-term antibacterial effects. Dental Materials. 2021; 37: 1248-1259.

[66] Kanwal N, Toms H, Hannon AC, Perras FA, Bryce DL, Karpukhina N, Abrahams I. Structure and solubility behaviour of zinc containing phosphate glasses. Journal of Materials Chemistry B. 2015, 3: 8842-8855.

[67] Refka O, Krimi S, Videau J, Khattech I, El Jazouli A, Jemal M. Structural and thermochemical study of $Na_2O–ZnO–P_2O_5$ glasses. Journal of Non-Crystalline Solids. 2014; 390: 5-12.

[68] Ahmed I, Lewis M, Olsen I, Knowles JC. Phosphate glasses for tissue engineering: Part 1. Processing and characterisation of a ternary-based $P_2O5–CaO–Na_2O$ glass system. Biomaterials. 2004; 25: 491-499.

[69] Pyare R, Lai LJ, Joshi VC, Singh VK. Leachability of molybdenum from ternary phosphate glasses. Journal of the American Ceramic Society. 1996; 79: 1329-1334.

[70] Liu G, Wu C, Abrams WR, Li Y. Structural and functional characteristics of the microbiome in deep-dentin caries. Journal of Dental Research. 2020; 99: 713-720.

[71] Kianoush N, Adler CJ, Nguyen KA, Browne GV, Simonian M, Hunter N. Bacterial profile of dentine caries and the impact of pH on bacterial population diversity. PLOS ONE. 2014; 9: e92940.

[72] Aas JA, Griffen AL, Dardis SR, Lee AM, Olsen I, Dewhirst FE, Leys EJ, Paster BJ. Bacteria of dental caries in primary and permanent teeth in children and young adults. Journal of Clinical Microbiology. 2008; 46: 1407-1417.

[73] Lima K, Coelho L, Pinheiro I, Rocas I, Siqueira Jr J. Microbiota of dentinal caries as assessed by reverse-capture checkerboard analysis. Caries Research. 2011; 45: 21-30.

[74] Hoshino E. Predominant obligate anaerobes in human carious dentin. Journal of Dental Research. 1985; 64: 1195-1198.

[75] Martin FE, Nadkarni MA, Jacques NA, Hunter N. Quantitative microbiological study of human carious dentine by culture and real-time PCR: association of anaerobes with histopathological changes in chronic pulpitis. Journal of Clinical Microbiology. 2002; 40: 1698-1704.

[76] Watanabe T, Hara Y, Yoshimi Y, Fujita Y, Yokoe M, Noguchi Y. Clinical characteristics of bloodstream infection by *Parvimonas micra*: retrospective case

series and literature review. BMC Infectious Diseases. 2020; 20: 578.

[77] Radman IK, Djeri A, Arbutina A, Milašin J. Microbiological findings in deep caries lesions. Serbia Dental Association. 2016; 63: 7-14.

[78] Blancas B, Lanzagorta ML, Jiménez-Garcia LF, Lara R, Molinari JL, Fernández AM. Study of the ultrastructure of *Enterococcus faecalis* and *Streptococcus mutans* incubated with salivary antimicrobial peptides. Clinical and Experimental Dental Research. 2021; 7: 365-375.

[79] Ramsey M, Hartke A, Huycke M. The physiology and metabolism of Enterococci. In: Gilmore MS, Clewell DB, Ike Y, Shankar N, editors. Enterococci: from commensals to leading causes of drug resistant infection. Boston: Massachusetts Eye and Ear Infirmary; 2014.

[80] Morey JR, Kehl-Fie TE. Bioinformatic mapping of opine-like zincophore biosynthesis in bacteria. mSystems. 2020; 5: e00554-20.

[81] Abrantes MC, Kok J, Silva Lopes MF. *Enterococcus faecalis* zinc-responsive proteins mediate bacterial defence against zinc overload, lysozyme and oxidative stress. Microbiology. 2014; 160: 2755-2762.

[82] Stuart CH, Schwartz SA, Beeson TJ, Owatz CB. *Enterococcus faecalis*: its role in root canal treatment failure and current concepts in retreatment. Journal of Endodontics. 2006; 32: 93-98.

[83] Hirose N, Kitagawa R, Kitagawa H, Maezono H, Mine A, Hayashi M, Haapasalo M, Imazato S. Development of a cavity disinfectant containing antibacterial monomer MDPB. Journal of Dental Research. 2016; 95: 1487-1493.

[84] Al-Nazhan S, Al-Sulaiman A, Al-Rasheed F, Alnajjar F, Al-Abdulwahab B, Al-Badah A. Microorganism penetration in dentinal tubules of instrumented and retreated root canal walls. *In vitro* SEM study. Restorative Dentistry & Endodontics. 2014; 39: 258.

[85] Zegadło K, Gieroń M, Żarnowiec P, Durlik-Popińska K, Kręcisz B, Kaca W, Czerwonka G. Bacterial motility and its role in skin and wound infections. International Journal of Molecular Sciences. 2023; 24: 1707.

[86] Gobbetti M, Minervini F. LACTOBACILLUS | *Lactobacillus casei*. In: Batt CA, Tortorello ML, editors. Encyclopedia of Food Microbiology (Second Edition). Oxford: Academic Press; 2014; 432-438.

[87] Chapter 3 - Supragingival Microbes. In: Zhou X, Li Y, editors. Atlas of Oral

Microbiology. Oxford: Academic Press; 2015: 41-65.

[88] Lenzi TL, Guglielmi Cde A, Arana-Chavez VE, Raggio DP. Tubule density and diameter in coronal dentin from primary and permanent human teeth. Microscopy and Microanalysis. 2013; 19: 1445-1449.

[89] Love RM, Jenkinson HF. Invasion of dentinal tubules by oral bacteria. Critical Reviews in Oral Biology & Medicine. 2002; 13: 171-183.

# TABLE LEGENDS

**Table 1. Mixing ratios of each component for preparing AG-1, AG-2 and AG-3**

**Table 2. Components of uncured resin.**

**Table 3. Results of X-ray fluorescence analysis of AG-1, AG-2, and AG-3.**

**Table 4. Bacteria and culture conditions.**

**Table 5. Minimum inhibitory concentrations (MICs) and minimum bactericidal concentrations (MBCs) of $Zn^{2+}$.**

# FIGURE LEGENDS

**Figure 1. Schematic diagram of acidity-responsive release of $Zn^{2+}$ and exhibition of on-demand antibacterial effects.**

**Figure 2. Schematic diagram of rapid release of $Zn^{2+}$ and exhibition of cavity disinfecting effects.**

**Figure 3. The protocol for evaluating on-demand ion-releasing property of Cont, AG-2, and AG-3.**

**Figure 4. The protocol for evaluating on-demand antibacterial activity of Cont, AG-2, and AG-3.**

**Figure 5. The protocol for evaluating on-demand antibacterial activity of dental resin incorporating 30 (wt)% AG-3.**

**Figure 6. The protocol for evaluating anti-biofilm effects of dental resin incorporating 30 (wt)% AG-3.**

**Figure 7. Field-emission scanning electron microscope images of AG-1 (A), AG-2 (B), and AG-3 (C).**

**Figure 8. X-ray diffraction patterns of AG-1 (A), AG-2 (B), and AG-3 (C).**

**Figure 9. Particle size distribution of AG-1 (A), AG-2 (B), and AG-3 (C).**

**Figure 10. Elemental mapping images of AG-1 (A), AG-2 (B), and AG-3 (C).**

**Figure 11. Solubility of Cont, AG-1, AG-2, and AG-3 in the pH-adjusted buffer solution (pH 7.0, 6.0, or 5.0)**

Bars represent the standard deviation of three replicates. Different letters (a-h) indicate significant differences ($p < 0.05$, ANOVA, Tukey's HSD test).

**Figure 12. Release of $Zn^{2+}$ (A) and $F^-$ (B) from Cont, AG-1, AG-2, and AG-3 exposed to pH-adjusted BHI broth (pH 7.0, 6.0, or 5.0).**

Bars represent the standard deviations of five replicates. Different letters (a-i) indicate significant differences ($p < 0.05$, ANOVA, Tukey's HSD test).

**Figure 13. Number of viable *S. mutans* after incubation in the presence of Cont, AG-1, AG-2, and AG-3.**

w/o: bacterial suspension without any glass. Bars represent the standard deviation of five replicates. Different letters (a-j) indicate significant differences ($p < 0.05$, ANOVA, Tukey's HSD test). Dashed line indicates the initial amount of bacteria.

**Figure 14. Release of $Zn^{2+}$ from Cont, AG-2, and AG-3 exposed to acetate buffer and HEPES.**

The concentration of $Zn^{2+}$ released into acetate buffer (pH 5.0) was measured on Day 1, 5, and 9. The concentration of $Zn^{2+}$ released into HEPES (pH7.0) was measured on Days 2 – 4 and Days 5 – 8.

Bars represent the standard deviation of three replicates.

**Figure 15. Number of *S. mutans* after incubation in the presence of Cont, AG-2, and AG-3 before and after two-time exposures to acetate buffer and HEPES.**

w/o: bacterial suspension without any glass. Bars represent the standard deviation of five replicates. Different letters (a-g) indicate significant differences ($p < 0.05$, ANOVA, Tukey's HSD test). Dashed line indicates the initial amount of bacteria.

**Figure 16. Number of viable *S. mutans* after incubation on the surface of dental resins incorporating 10, 20, and 30 (wt)% of AG-3.**

Bars represent the standard deviations of three replicates. Different letters (a-g) indicate significant difference ($p < 0.05$, ANOVA, Tukey's HSD test). Dashed line indicates the initial amount of bacteria.

**Figure 17. Release of $Zn^{2+}$ from dental resin incorporating 30 (wt)% of AG-3 exposed to acetate buffer and HEPES.**

The concentration of $Zn^{2+}$ released into acetate buffer (pH 5.0) was measured on Day 1, 5, and 9. The concentration of $Zn^{2+}$ released into HEPES (pH7.0) was measured on Days 2 – 4 and Days 5 – 8. Bars represent the standard deviation of three replicates.

**Figure 18. SEM images of dental resin incorporating 30 (wt)% AG-3 before exposure to buffer solution (Day 0) (A, B) and after the third exposure to acetate buffer (Day 9) (C, D).**

Scale bar, 50 μm (A, C); 5 μm (B, D).

**Figure 19. Number of viable *S. mutans* after incubation on the surface of dental resin incorporating 30 (wt)% of AG-3 before and after two-time exposures to acetate buffer and HEPES.**

Bars represent the standard deviation of three replicates. * indicates significant difference ($p < 0.05$, student's *t*-test). Dashed line indicates the initial amount of bacteria.

**Figure 20. SEM images of biofilm formed on control resin (A) and dental resin incorporating 30 (wt)% AG-3 (B) after the third exposure to acetate buffer.**

Scale bar, 5 μm.

Arrow indicates that the morphology of bacteria was observed to be disrupted.

**Figure 21. Thickness of biofilm (A) and percentage of membrane-compromised bacteria (B) analyzed from CLSM images of *S. mutans* biofilm.**

Bars represent the standard deviation of three replicates. * indicates significant difference ($p < 0.05$, student's *t*-test).

**Figure 22. The protocol for evaluating antibacterial activity of dental resin incorporating 10 (wt)% RG in dentinal tubules.**

**Figure 23. Field-emission scanning electron microscope (A) and elemental mapping (B) images of RG.**

**Figure 24. Particle size distribution (A) and X-ray diffraction patterns (B) of RG.**

**Figure 25. Solubility of RG in the pH-adjusted buffer solution (pH 7.0, 6.0, or 5.0).**

Bars represent the standard deviation of five replicates. * indicates significant differences ($p < 0.05$, ANOVA, Tukey's HSD test).

**Figure 26. Release of $Zn^{2+}$ from RG exposed to pH-adjusted BHI broth (pH 7.0, 6.0, or 5.0).**

Bars represent the standard deviations of five replicates. * indicates significant differences ($p < 0.05$, ANOVA, Tukey's HSD test).

**Figure 27. Number of viable bacteria after incubation in the presence of RG.**

(-): After incubation in the absence of RG. (+): After incubation in the presence of RG. Arrows indicate 100% killing effect. Bars represent the standard deviations of five replicates. * indicates significant differences ($p < 0.05$, Student's *t*-test). Dashed line indicates the initial amount of bacteria.

**Figure 28. CLSM images of *L. casei*-infected dentin model (A), *L. casei*-infected dentin model treated by dental resin incorporating 10 (wt)% RG under the dry condition (B), *L. casei*-infected dentin model treated by dental resin incorporating 10 (wt)% RG under the wet condition (C), and *L. casei*-infected dentin model treated by control resin without RG (D) after LIVE/DEAD staining.**

Scale bar, 50 μm.

**Figure 29. CLSM images of *S. mutans*-infected dentin model (A), *S. mutans*-infected dentin model treated by dental resin incorporating 10 (wt)% RG under the dry condition (B), *S. mutans*-infected dentin model treated by dental resin incorporating 10 (wt)% RG under the wet condition (C), and *S. mutans*-infected dentin model treated by control resin without RG (D) after LIVE/DEAD staining.** Scale bar, 50 μm.

**Table 1. Mixing ratios of components for preparing AG-1, AG-2 and AG-3.**

| Glass / Components | AG-1 | AG-2 | AG-3 |
|---|---|---|---|
| $SiO_2$ | 45.7 | 35.5 | 30.5 |
| ZnO | 23.0 | 33.2 | 38.2 |
| $Na_2O$ | 5.0 | 5.0 | 5.0 |
| F | 18.7 | 18.7 | 18.7 |
| Others | 7.6 | 7.6 | 7.6 |

(mol%)

**Table 2. Components of uncured resin.**

| Components | Function | wt% |
|---|---|---|
| Triethylene glycol dimethacrylate (TEGDMA) | Monomer | 89.0 |
| 2-hydroxyethyl methacrylate (HEMA) | Monomer | 10.0 |
| Camphorquinone (CQ) | Initiator | 0.3 |
| Ethyl p-dimethylaminobenzoate (EPA) | Reducing agent | 0.6 |
| 2,6-di-tert-butyl-p-benzoyl (BHT) | Inhibitor | 0.1 |

**Table 3. Results of X-ray fluorescence analysis of AG-1, AG-2, and AG-3.**

| Glass / Components | AG-1 | AG-2 | AG-3 |
|---|---|---|---|
| $SiO_2$ | 42.9 | 33.4 | 29.2 |
| ZnO | 25.3 | 34.6 | 42.7 |
| $Na_2O$ | 7.1 | 7.8 | 9.2 |
| F | 17.0 | 16.0 | 10.5 |
| Others | 7.7 | 8.2 | 8.4 |

(mol%)

**Table 4. Bacteria and culture conditions.**

| Species | Broth | Agar |
|---|---|---|
| *Lactobacillus casei* ATCC4646 | Lactobacilli Inoculum Broth | Lactobacilli Inoculum Broth plates supplemented with 1.5% Bacto agar |
| *Actinomyces naeslundii* ATCC19246 | Brain Heart Infusion Broth | Brain Heart Infusion agar |
| *Enterococcus faecalis* SS497 | Brain Heart Infusion Broth | Brain Heart Infusion agar |
| *Fusobacterium nucleatum* 1436 | Todd Hewitt Broth containing 0.1% L-cysteine | Todd Hewitt Broth agar containing 0.1% L-cysteine |
| *Parvimonas micra* GIFU7745 | Brain Heart Infusion Broth | Brain Heart Infusion agar |
| *Streptococcus mutans* NCTC10449 | Brain Heart Infusion Broth | Brain Heart Infusion agar |

**Table 5. Minimum inhibitory concentrations (MICs) and minimum bactericidal concentrations (MBCs) of $Zn^{2+}$.**

| | MIC | MBC |
|---|---|---|
| *Lactobacillus casei* ATCC4646 | 500 | 2000 |
| *Actinomyces naeslundii* ATCC19246 | 62.5 | 125 |
| *Enterococcus faecalis* SS497 | 1000 | 4000 |
| *Fusobacterium nucleatum* 1436 | 125 | 500 |
| *Parvimonas micra* GIFU7745 | 125 | 250 |
| **Streptococcus mutans* NCTC10449 | 125 | 250 |

(ppm)

* Data extrapolated from Experiment 1.

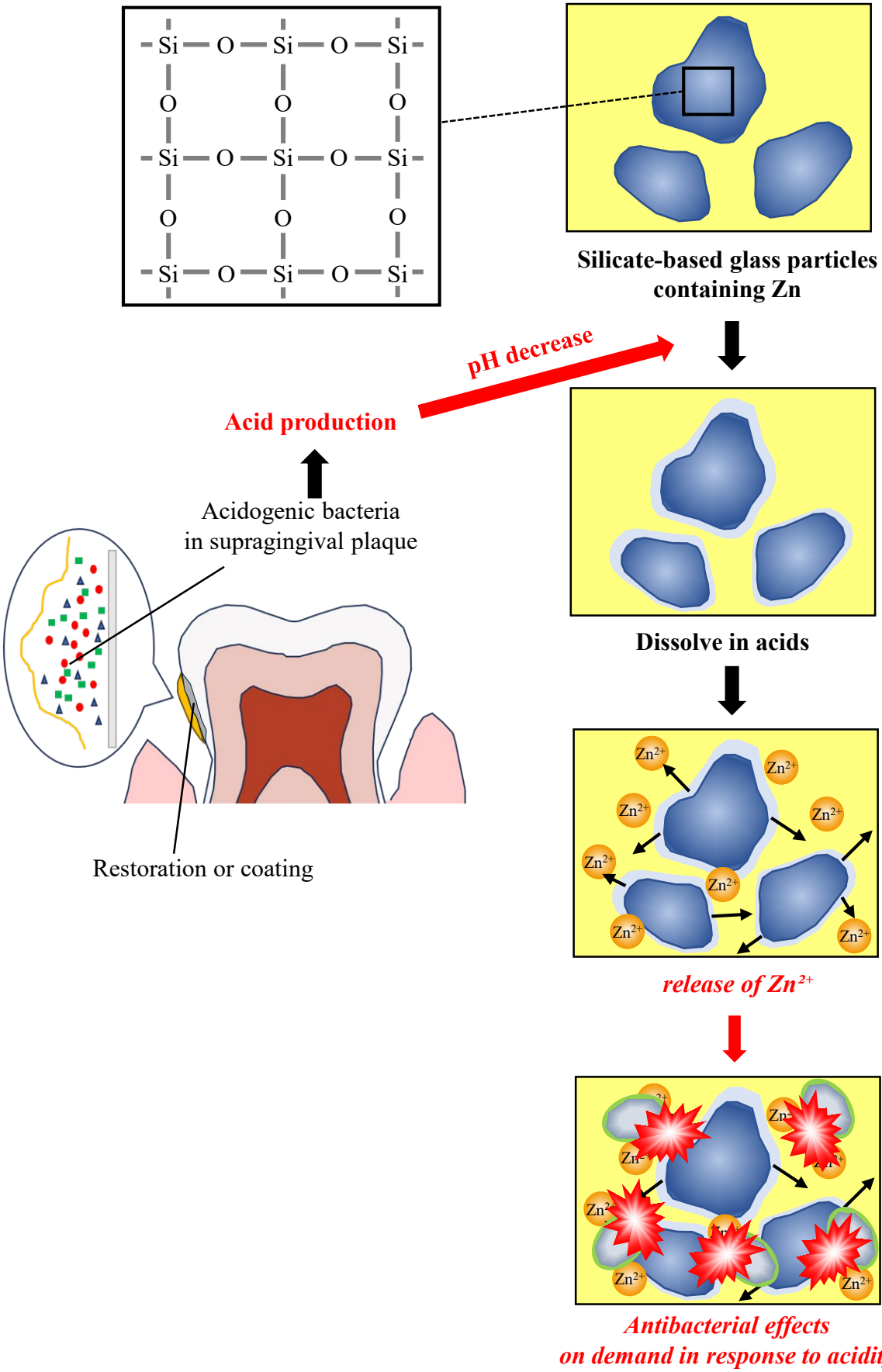


**Figure 1. Schematic diagram of acidity-responsive release of $Zn^{2+}$ and exhibition of on-demand antibacterial effects.**

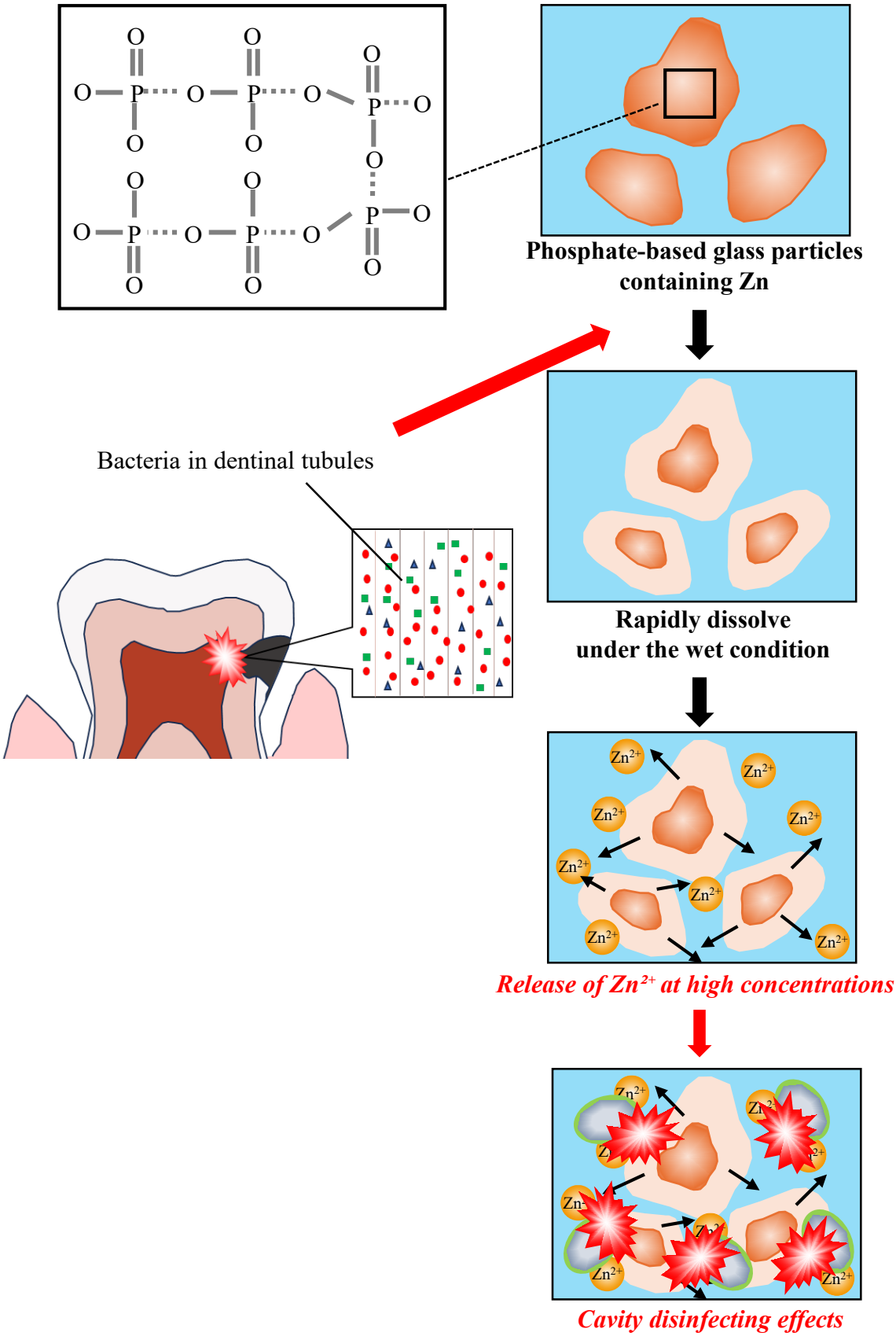


**Figure 2. Schematic diagram of rapid release of $Zn^{2+}$ and exhibition of cavity disinfecting effects.**

| Day 0-1 | Day 1-2 | Day 2-3 | Day 3-4 | Day 4-5 | Day 5-6 | Day 6-7 | Day 7-8 | Day 8-9 |
|---|---|---|---|---|---|---|---|---|
| **Acetate buffer (pH 5.0)** | HEPES (pH 7.0) | HEPES (pH 7.0) | HEPES (pH 7.0) | **Acetate buffer (pH 5.0)** | HEPES (pH 7.0) | HEPES (pH 7.0) | HEPES (pH 7.0) | **Acetate buffer (pH 5.0)** |

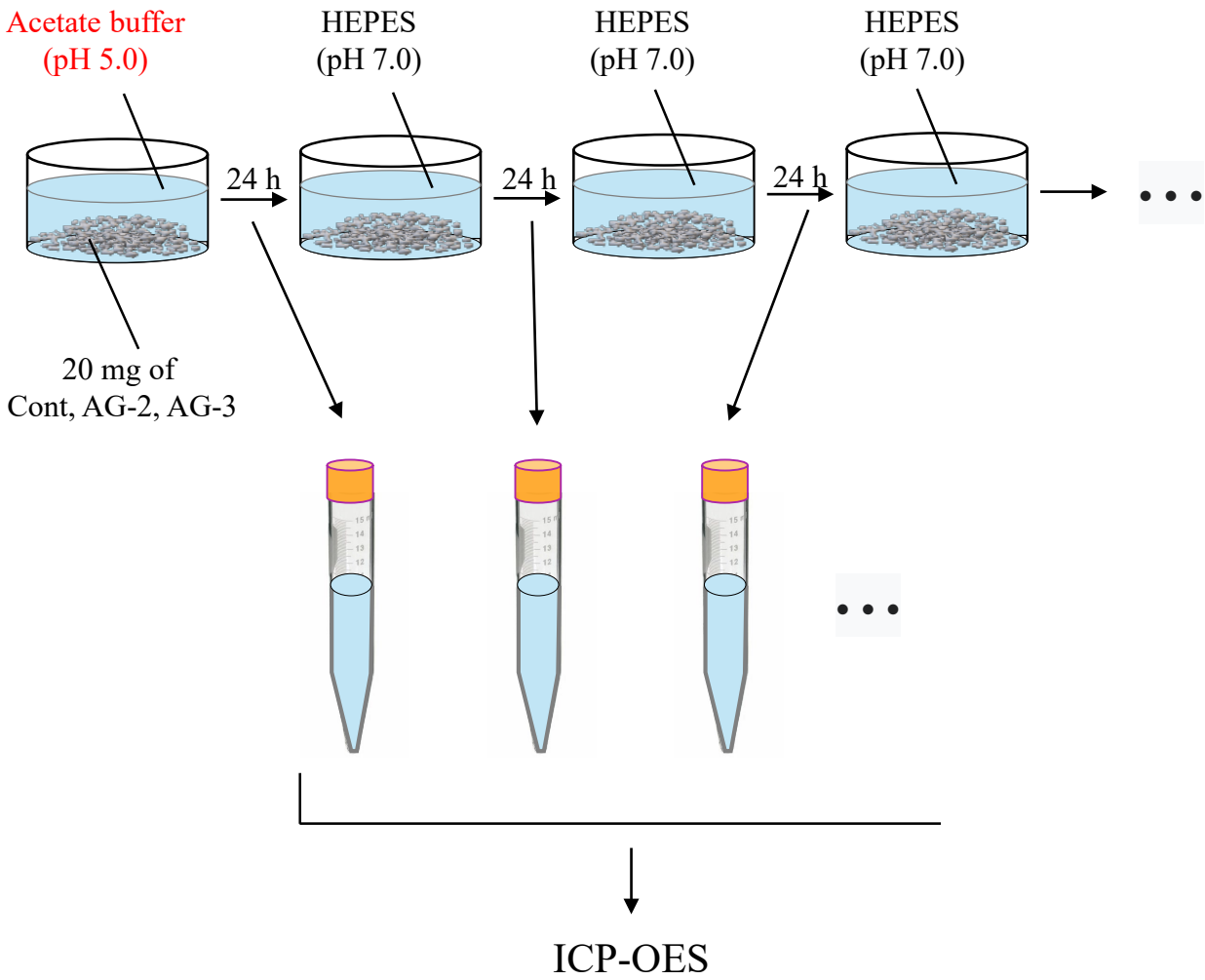


**Figure 3. The protocol for evaluating on-demand ion-releasing property of Cont, AG-2, and AG-3.**

| Day 0-1 | Day 1-2 | Day 2-3 | Day 3-4 | Day 4-5 | Day 5-6 | Day 6-7 | Day 7-8 | Day 8-9 |
|---|---|---|---|---|---|---|---|---|
| Acetate buffer (pH 5.0) | HEPES (pH 7.0) | HEPES (pH 7.0) | HEPES (pH 7.0) | Acetate buffer (pH 5.0) | HEPES (pH 7.0) | HEPES (pH 7.0) | HEPES (pH 7.0) | ***S. mutans*** **(pH 7.0/5.0)** |

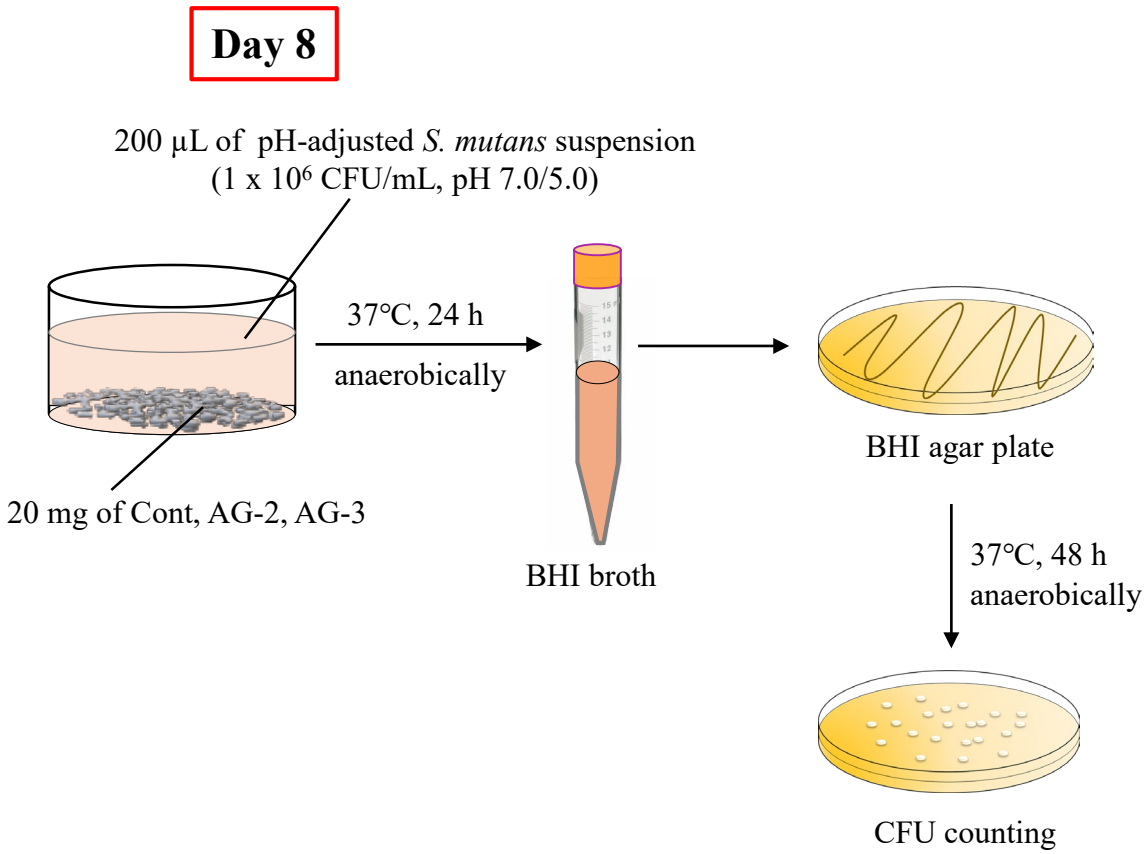


**Figure 4. The protocol for evaluating on-demand antibacterial activity of Cont, AG-2, and AG-3.**

| Day 0-1 | Day 1-2 | Day 2-3 | Day 3-4 | Day 4-5 | Day 5-6 | Day 6-7 | Day 7-8 | Day 8-9 |
|---|---|---|---|---|---|---|---|---|
| Acetate buffer (pH 5.0) | HEPES (pH 7.0) | HEPES (pH 7.0) | HEPES (pH 7.0) | Acetate buffer (pH 5.0) | HEPES (pH 7.0) | HEPES (pH 7.0) | HEPES (pH 7.0) | ***S. mutans*** **(pH 7.0/5.0)** |

**Day 8**

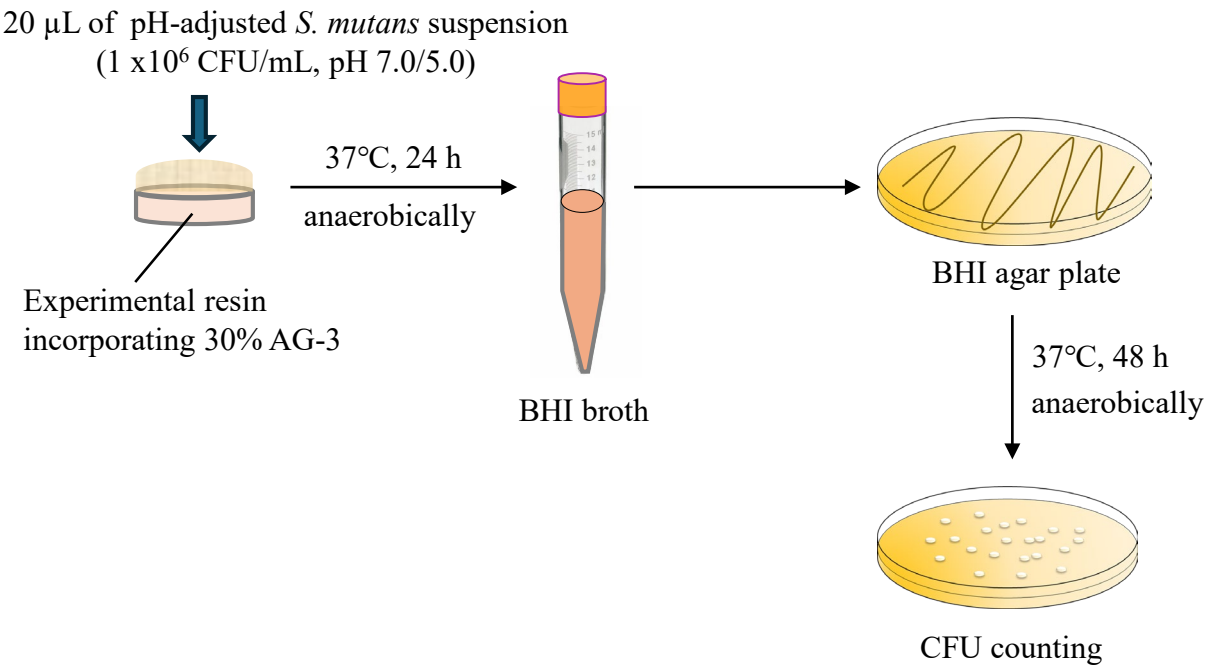


**Figure 5. The protocol for evaluating on-demand antibacterial activity of dental resin incorporating 30 (wt)% AG-3.**

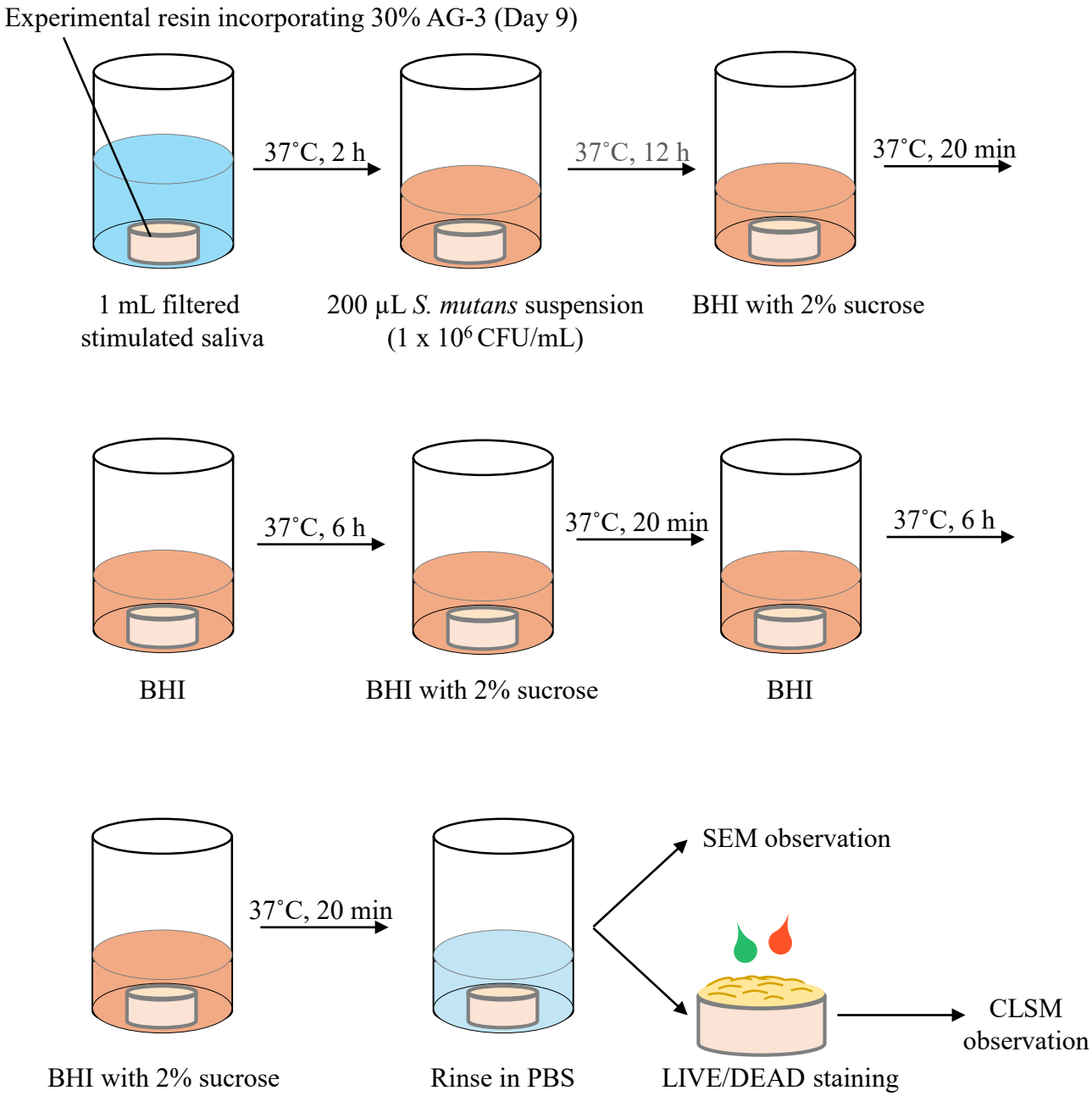


**Figure 6. The protocol for evaluating anti-biofilm effects of dental resin incorporating 30 (wt)% AG-3.**

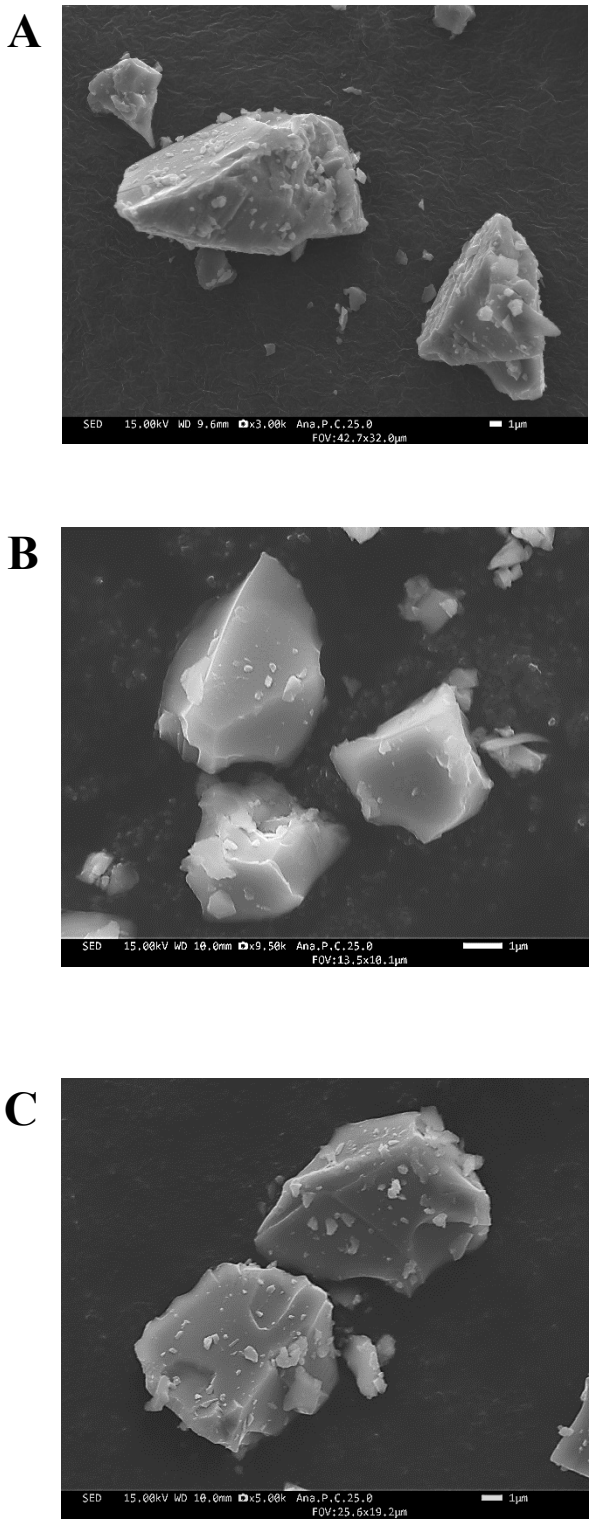


**Figure 7. Field-emission scanning electron microscope images of AG-1 (A), AG-2 (B), and AG-3 (C).**

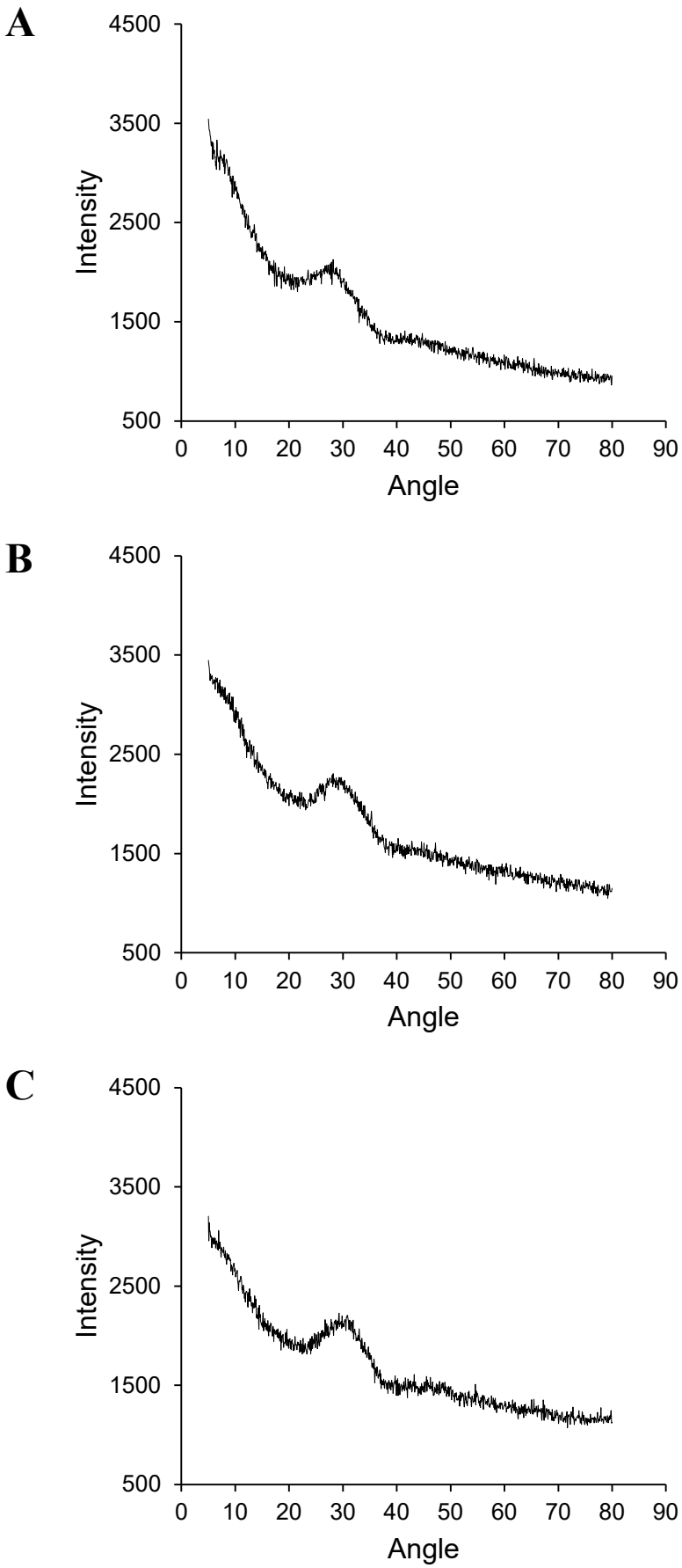


**Figure 8. X-ray diffraction patterns of AG-1 (A), AG-2 (B), and AG-3 (C).**

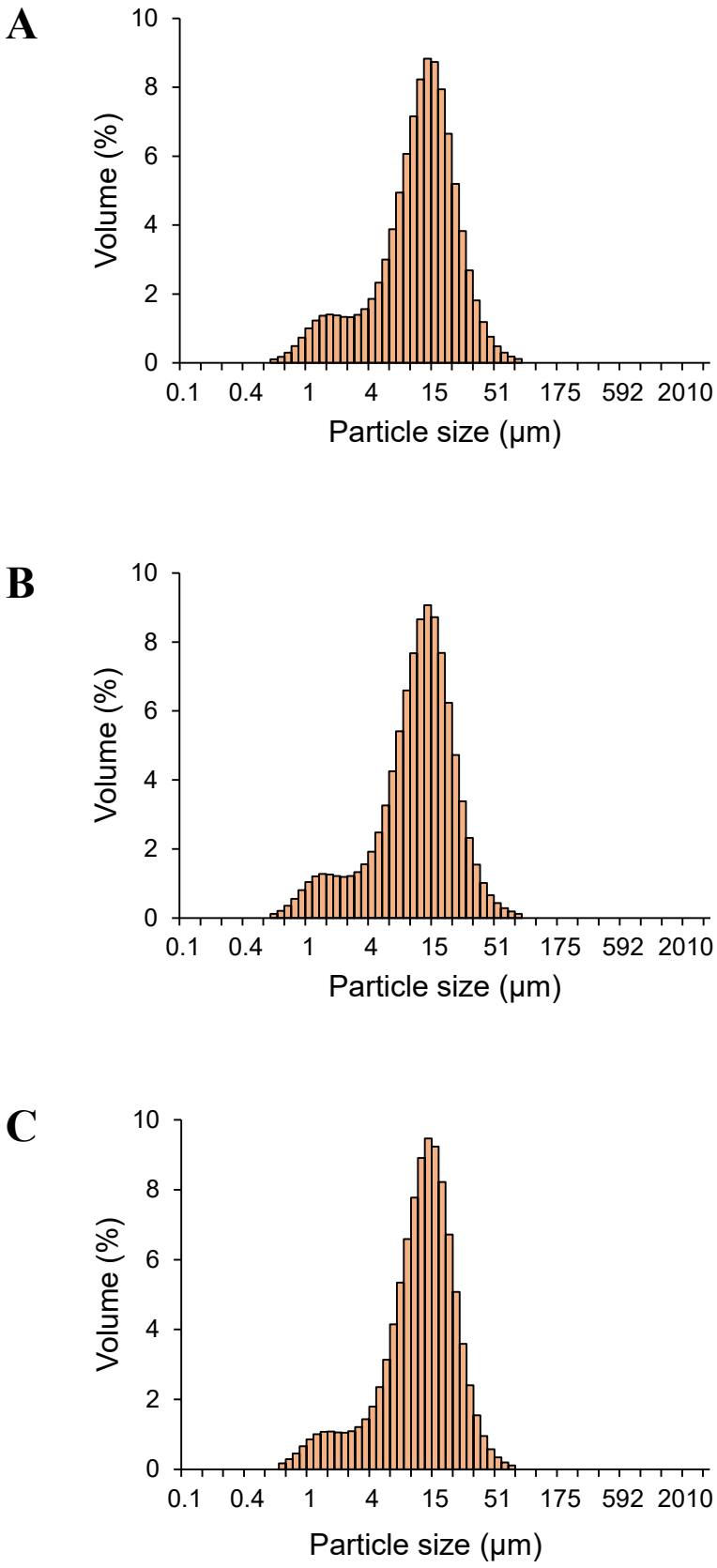


**Figure 9. Particle size distribution of AG-1 (A), AG-2 (B), and AG-3 (C).**

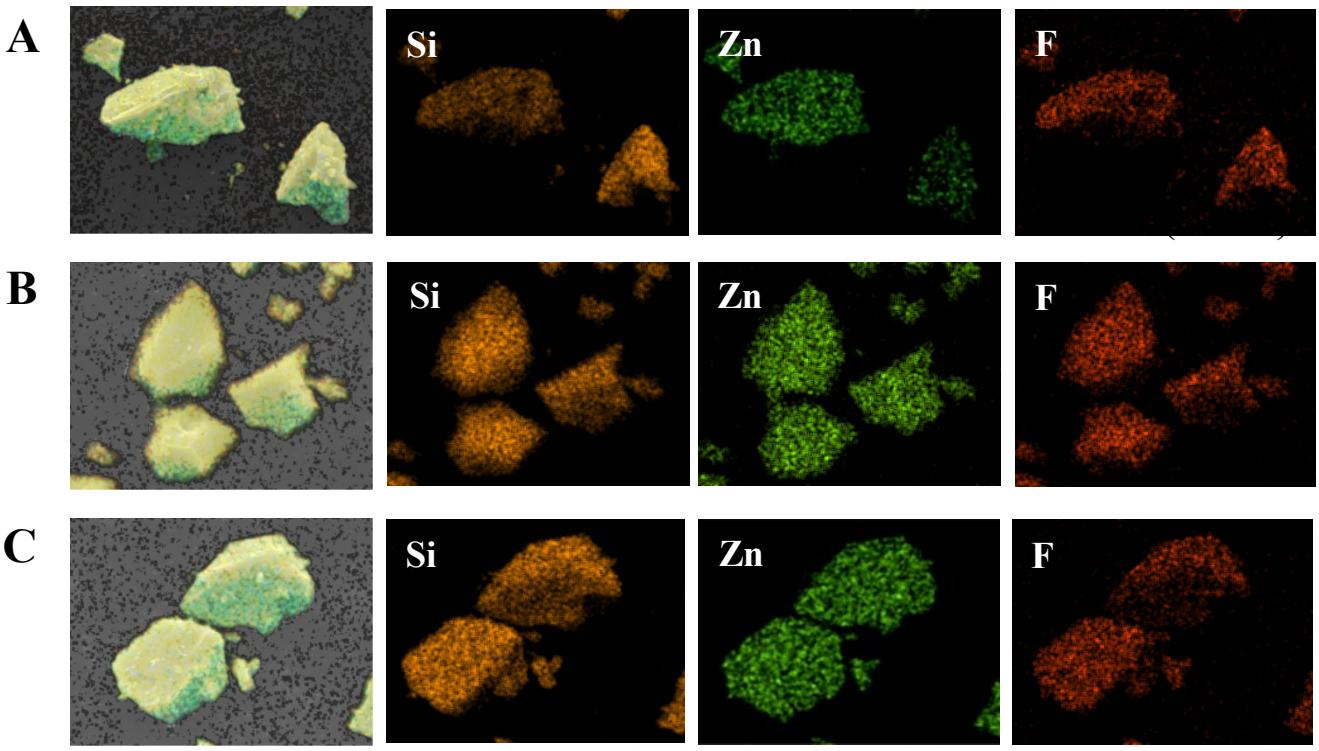


**Figure 10. Elemental mapping images of AG-1 (A), AG-2 (B), and AG-3 (C).**

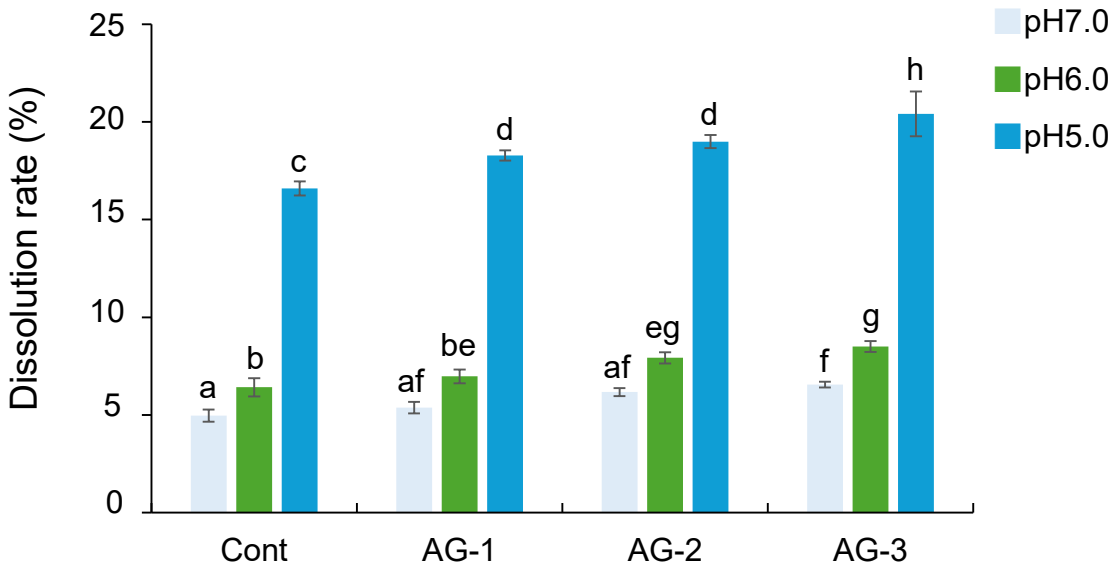


**Figure 11. Solubility of Cont, AG-1, AG-2, and AG-3 in the pH-adjusted buffer solution (pH 7.0, 6.0, or 5.0).**

Bars represent the standard deviation of three replicates. Different letters (a-h) indicate significant differences ($p < 0.05$, ANOVA, Tukey's HSD test).

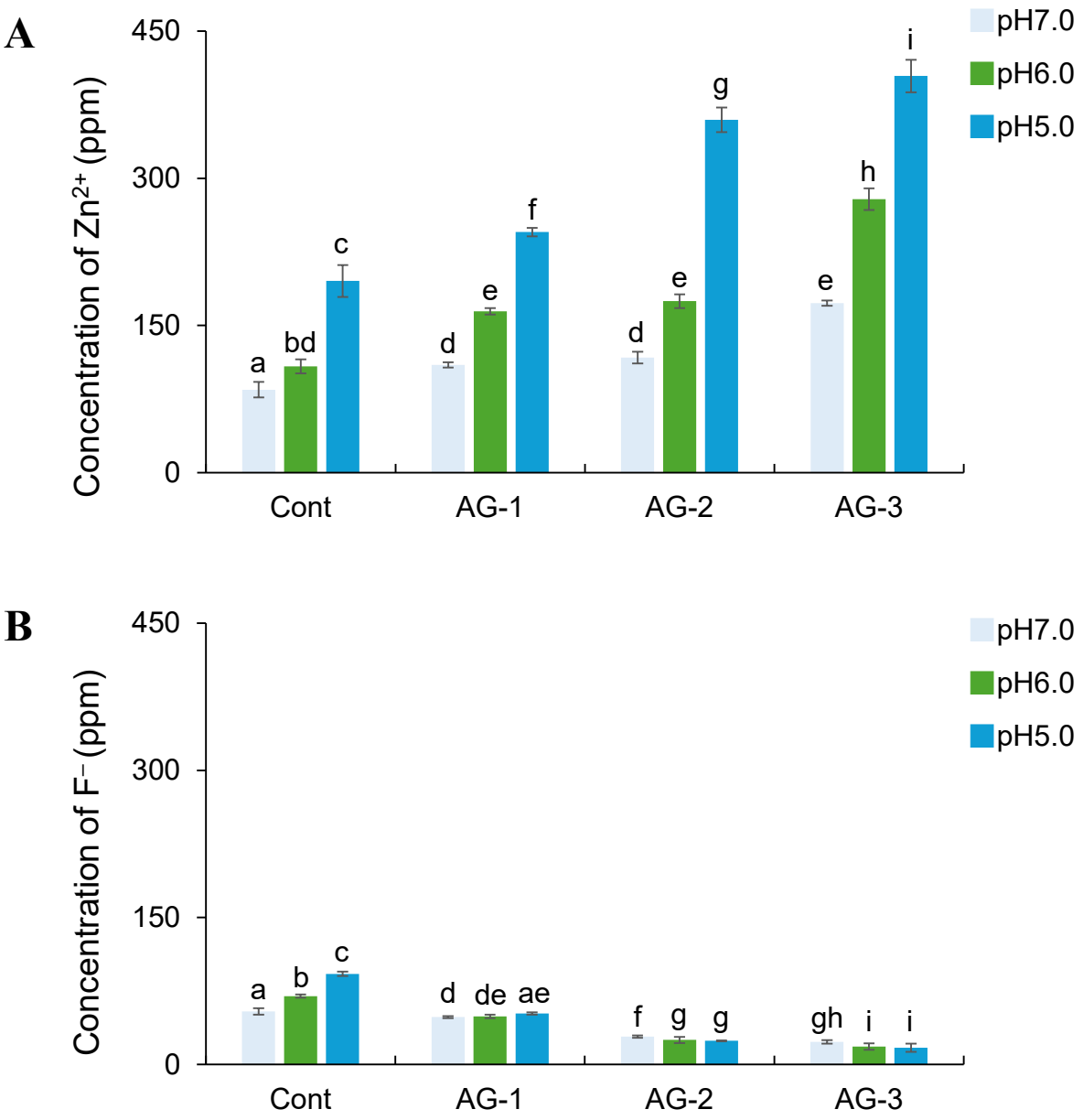


**Figure 12. Release of $Zn^{2+}$ (A) and $F^-$ (B) from Cont, AG-1, AG-2, and AG-3 exposed to pH-adjusted BHI broth (pH 7.0, 6.0, or 5.0).**

Bars represent the standard deviations of five replicates. Different letters (a-i) indicate significant differences ($p < 0.05$, ANOVA, Tukey's HSD test).

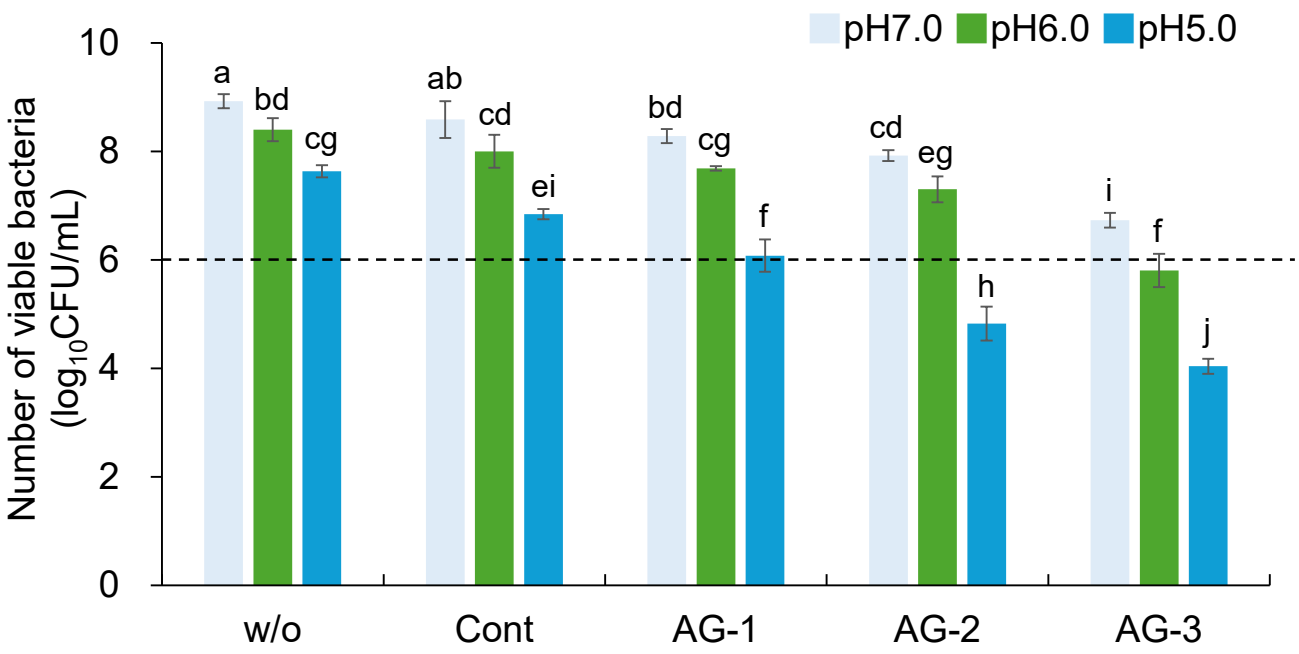


**Figure 13. Number of viable *S. mutans* after incubation in the presence of Cont, AG-1, AG-2, and AG-3.**

w/o: bacterial suspension without any glass. Bars represent the standard deviation of five replicates. Different letters (a-j) indicate significant differences ($p < 0.05$, ANOVA, Tukey's HSD test). Dashed line indicates the initial amount of bacteria.

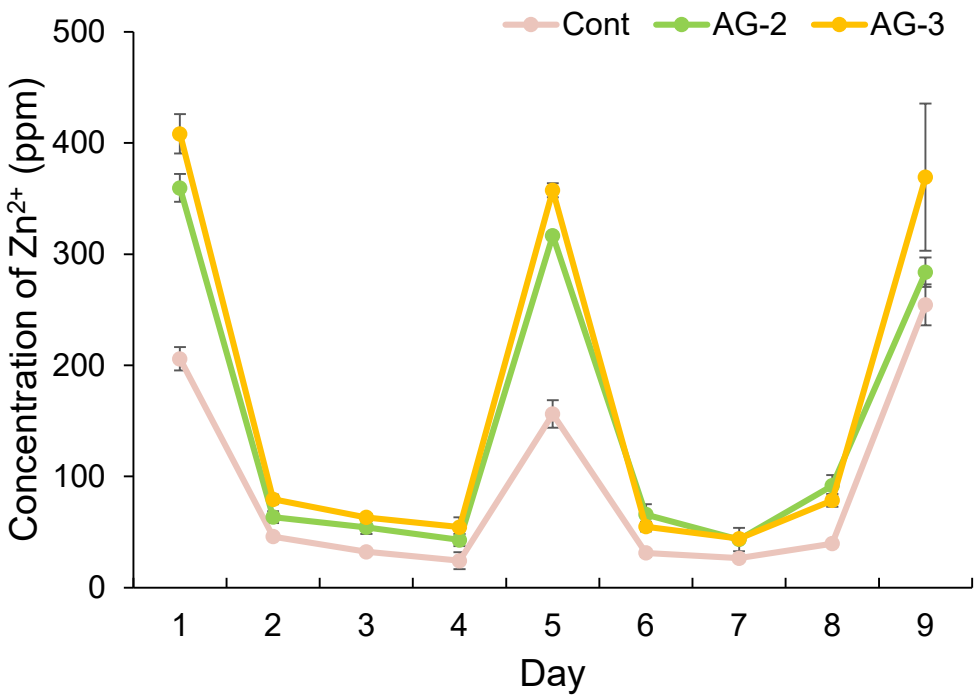


**Figure 14. Release of $Zn^{2+}$ from Cont, AG-2, and AG-3 exposed to acetate buffer and HEPES.**

The concentration of $Zn^{2+}$ released into acetate buffer (pH 5.0) was measured on Day 1, 5, and 9. The concentration of $Zn^{2+}$ released into HEPES (pH7.0) was measured on Days 2 – 4 and Days 5 – 8.

Bars represent the standard deviation of three replicates.

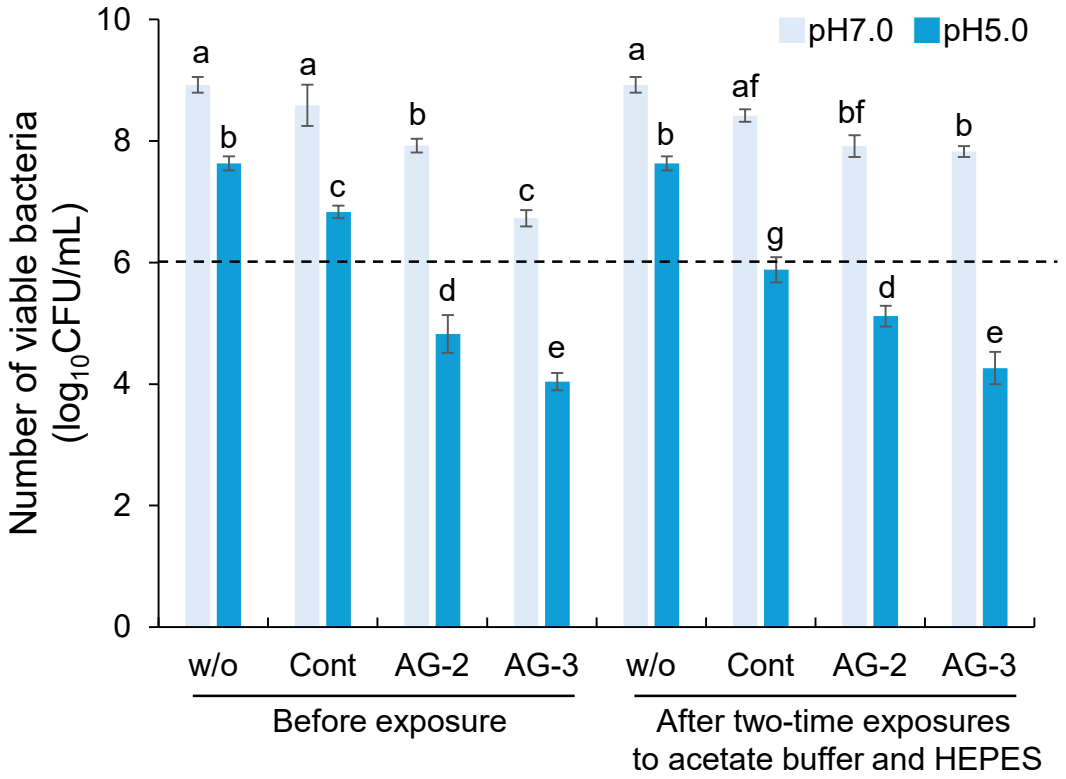


**Figure 15. Number of viable *S. mutans* after incubation in the presence of Cont, AG-2, and AG-3 before and after two-time exposures to acetate buffer and HEPES.**

w/o: bacterial suspension without any glass. Bars represent the standard deviation of five replicates. Different letters (a-g) indicate significant differences ($p < 0.05$, ANOVA, Tukey's HSD test). Dashed line indicates the initial amount of bacteria.

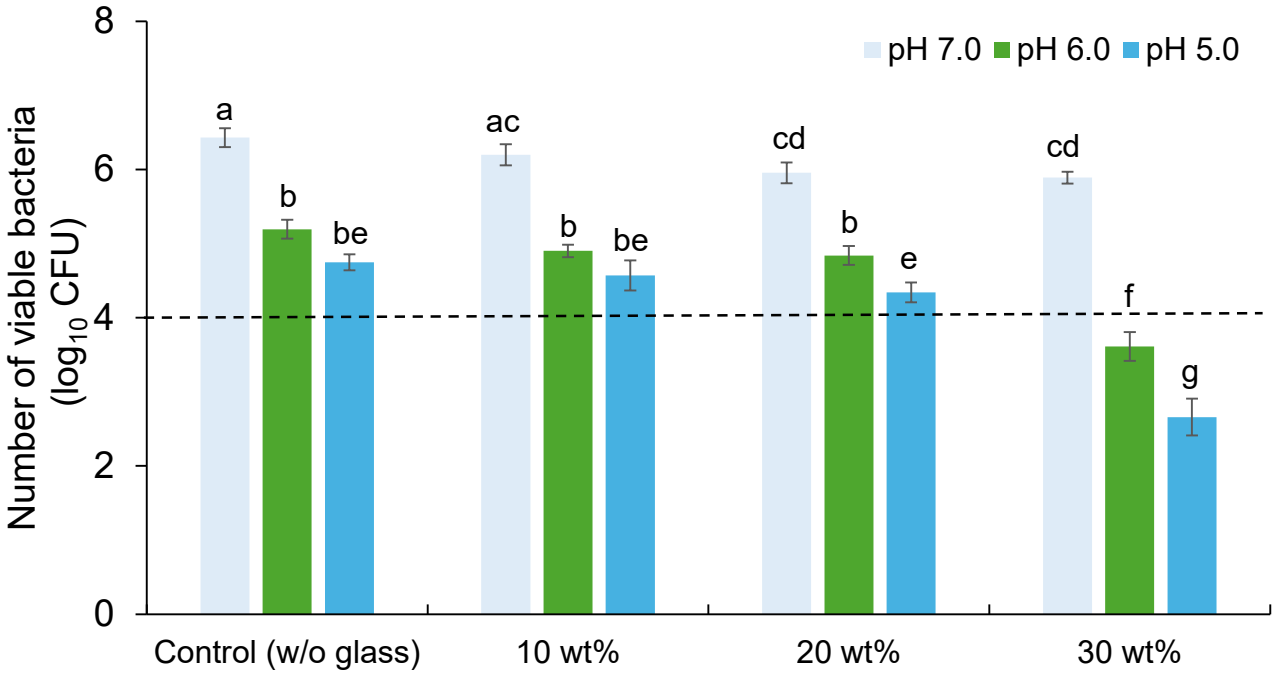


**Figure 16. Number of viable *S. mutans* after incubation on the surface of dental resins incorporating 10, 20, and 30 (wt)% AG-3.**

Bars represent the standard deviations of three replicates. Different letters (a-g) indicate significant difference ($p < 0.05$, ANOVA, Tukey's HSD test). Dashed line indicates the initial amount of bacteria.

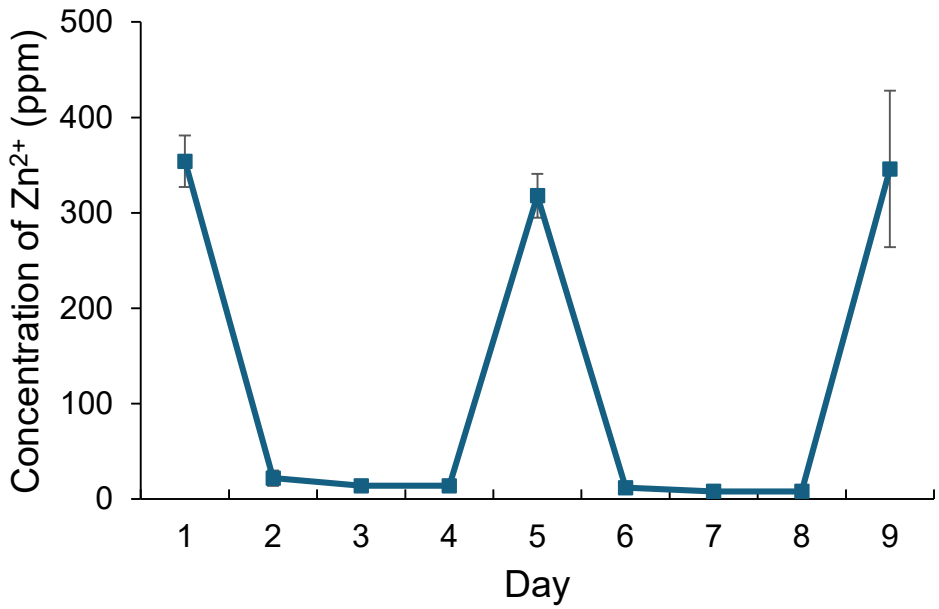


**Figure 17. Release of $Zn^{2+}$ from dental resin incorporating 30 (wt)% AG-3 exposed to acetate buffer and HEPES.**

The concentration of $Zn^{2+}$ released into acetate buffer (pH 5.0) was measured on Day 1, 5, and 9. The concentration of $Zn^{2+}$ released into HEPES (pH7.0) was measured on Days 2 – 4 and Days 5 – 8. Bars represent the standard deviation of three replicates.

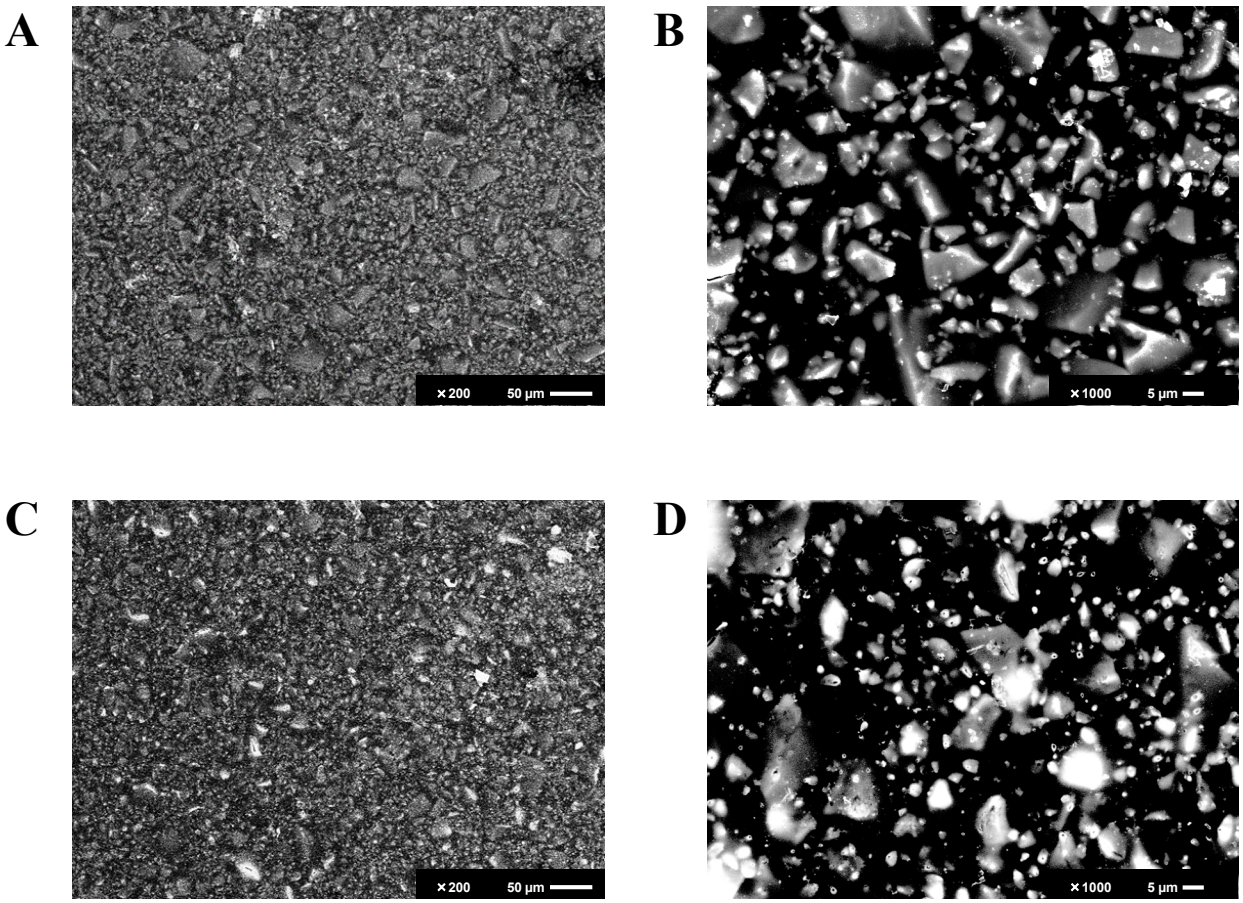


**Figure 18. SEM images of dental resin incorporating 30 (wt)% AG-3 before exposure to buffer solution (Day 0) (A, B) and after the third exposure to acetate buffer (Day 9) (C, D).** Scale bar, 50 µm (A, C); 5 µm (B, D).

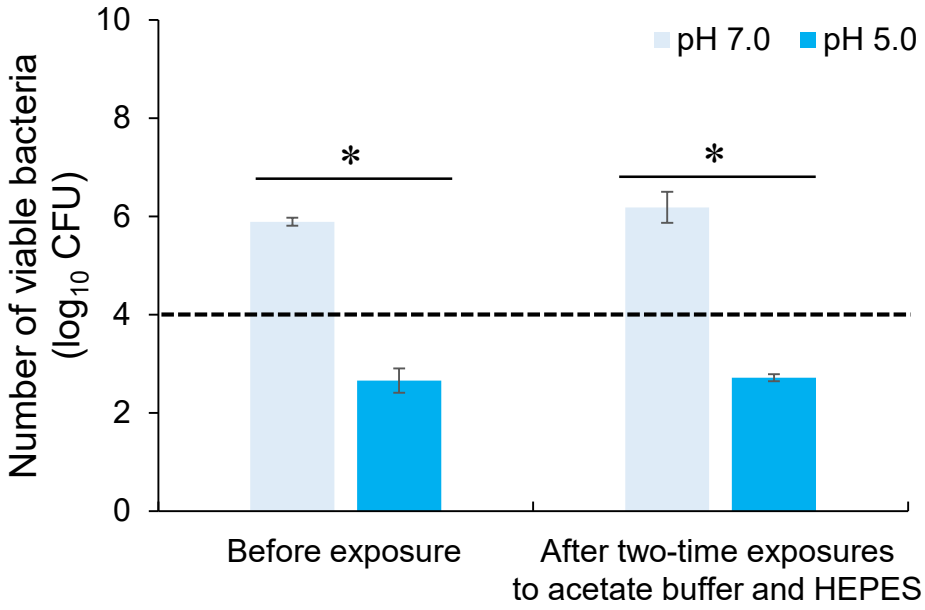


**Figure 19. Number of viable *S. mutans* after incubation on the surface of dental resin incorporating 30 (wt)% AG-3 before and after two-time exposures to acetate buffer and HEPES.** Bars represent the standard deviation of three replicates. * indicates significant difference ($p < 0.05$, student's *t*-test). Dashed line indicates the initial amount of bacteria.

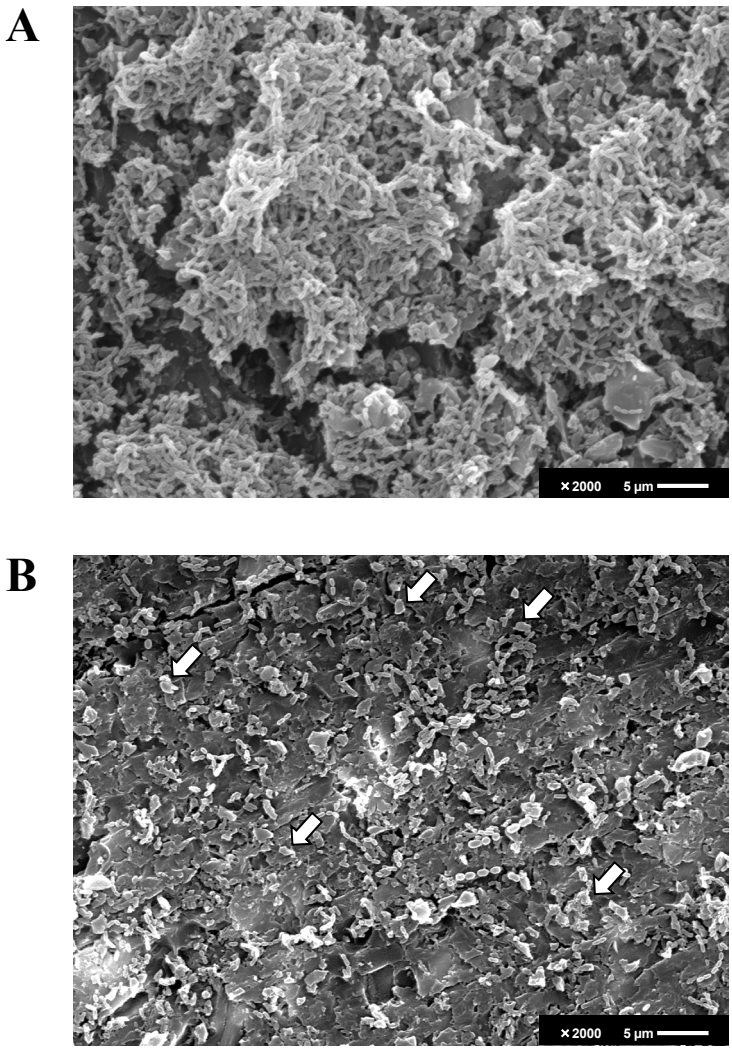


**Figure 20. SEM images of biofilm formed on control resin (A) and dental resin incorporating 30 (wt)% AG-3 (B) after the third exposure to acetate buffer.**

Scale bar, 5 μm.

Arrow: The morphology of bacteria was observed to be disrupted.

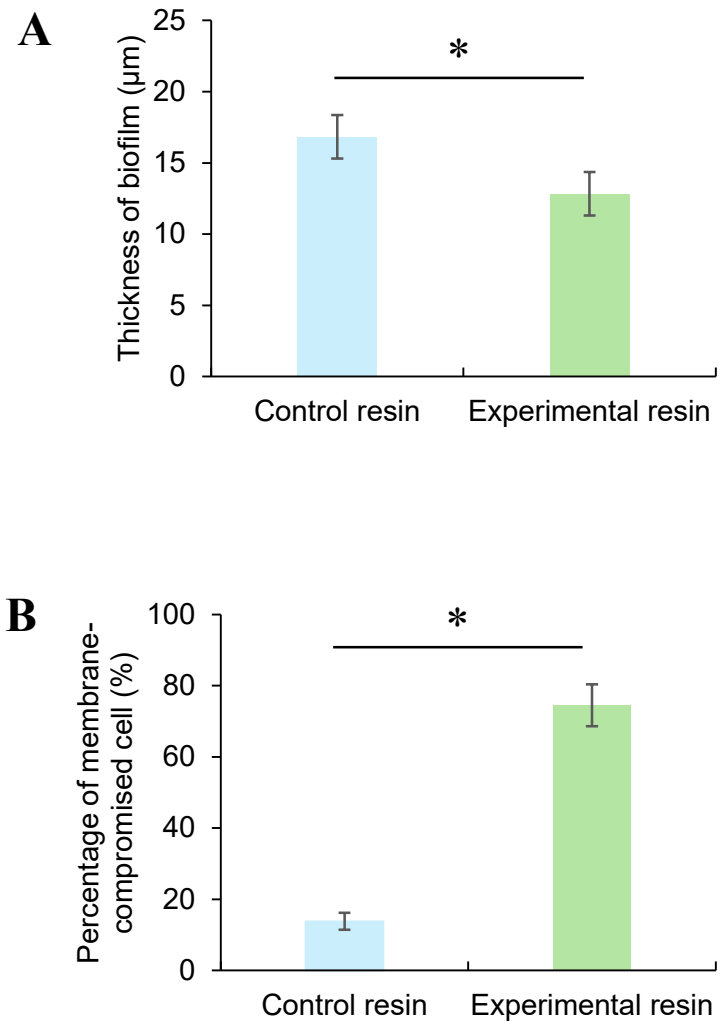


**Figure 21. Thickness of biofilm (A) and percentage of membrane-compromised bacteria (B) analyzed from CLSM images of *S. mutans* biofilm.**

Bars represent the standard deviation of three replicates. * indicates significant difference ($p < 0.05$, student's *t*-test).

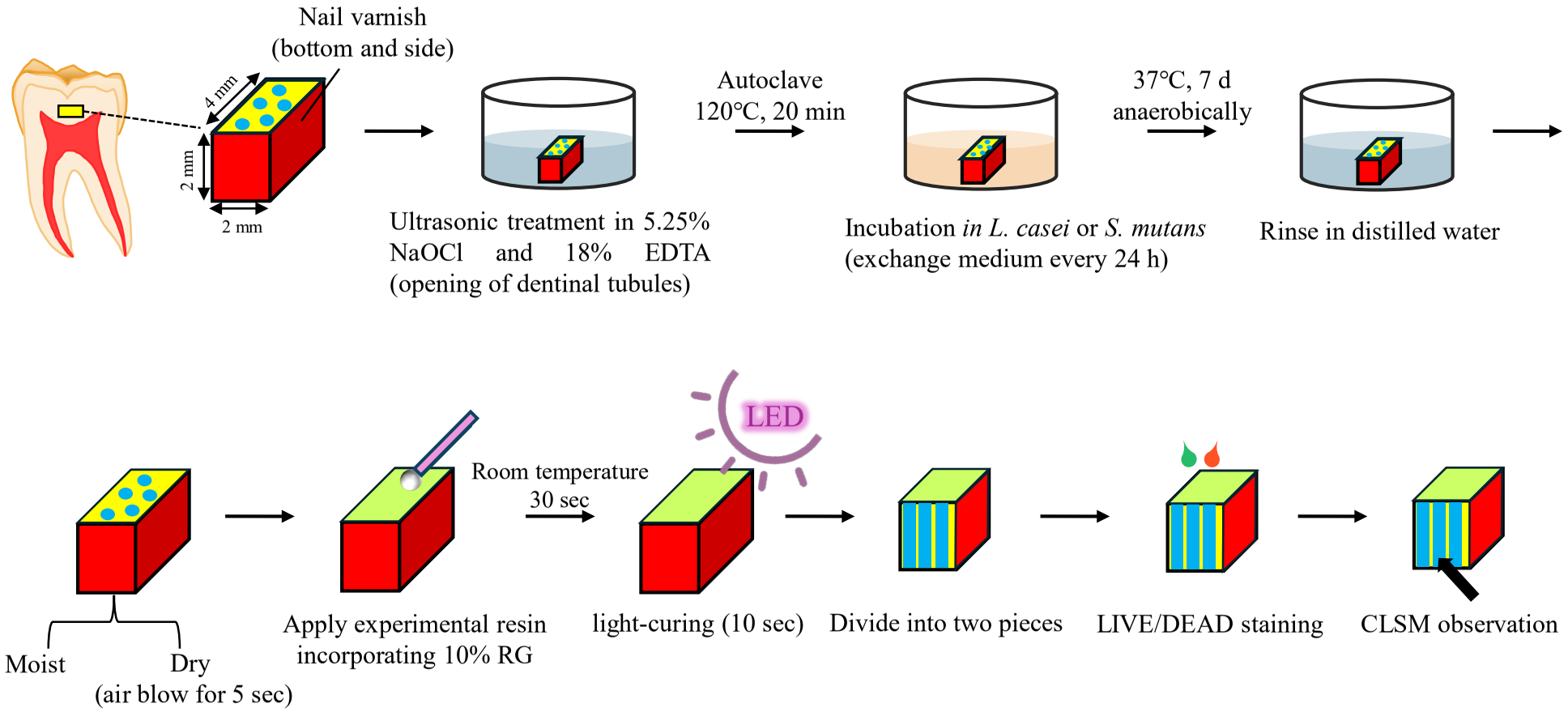


**Figure 22. The protocol for evaluating antibacterial activity of dental resin incorporating 10 (wt)% RG in dentinal tubules.**

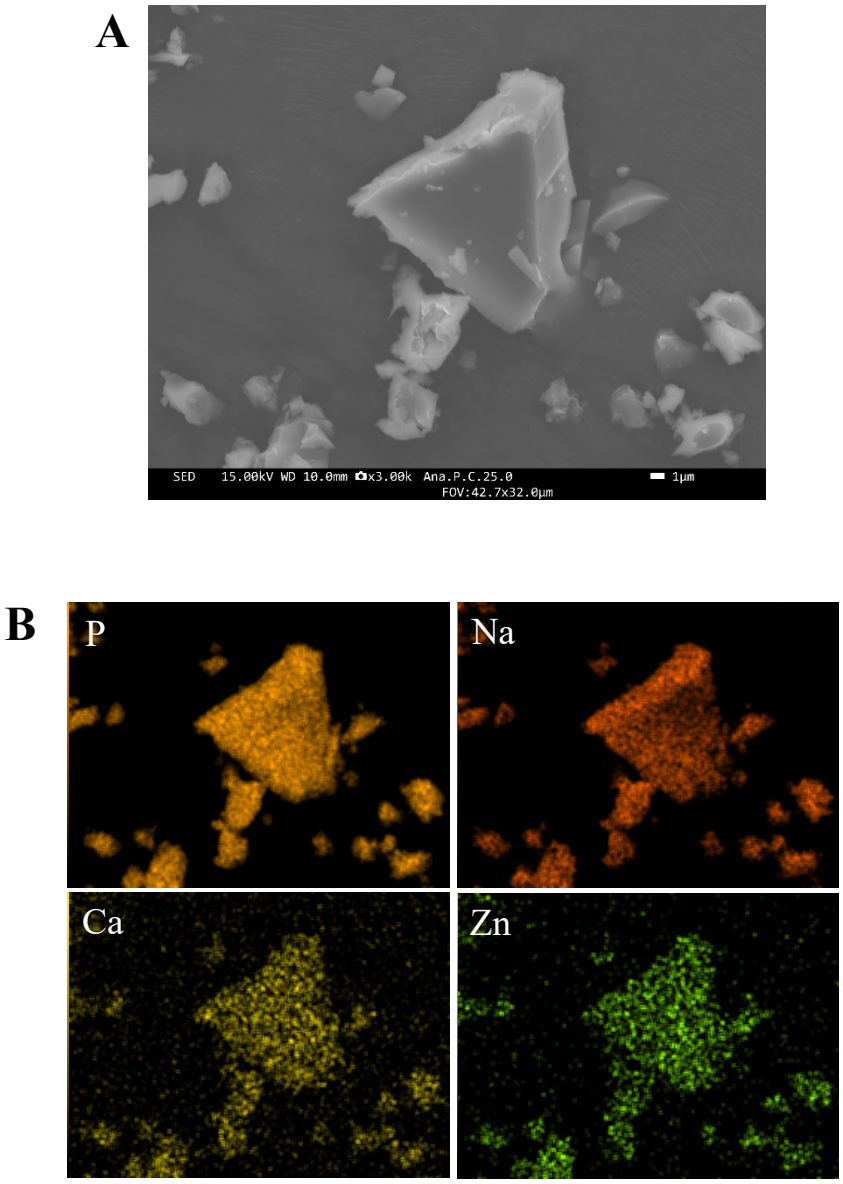


**Figure 23. Field-emission scanning electron microscope (A) and elemental mapping (B) images of RG.**

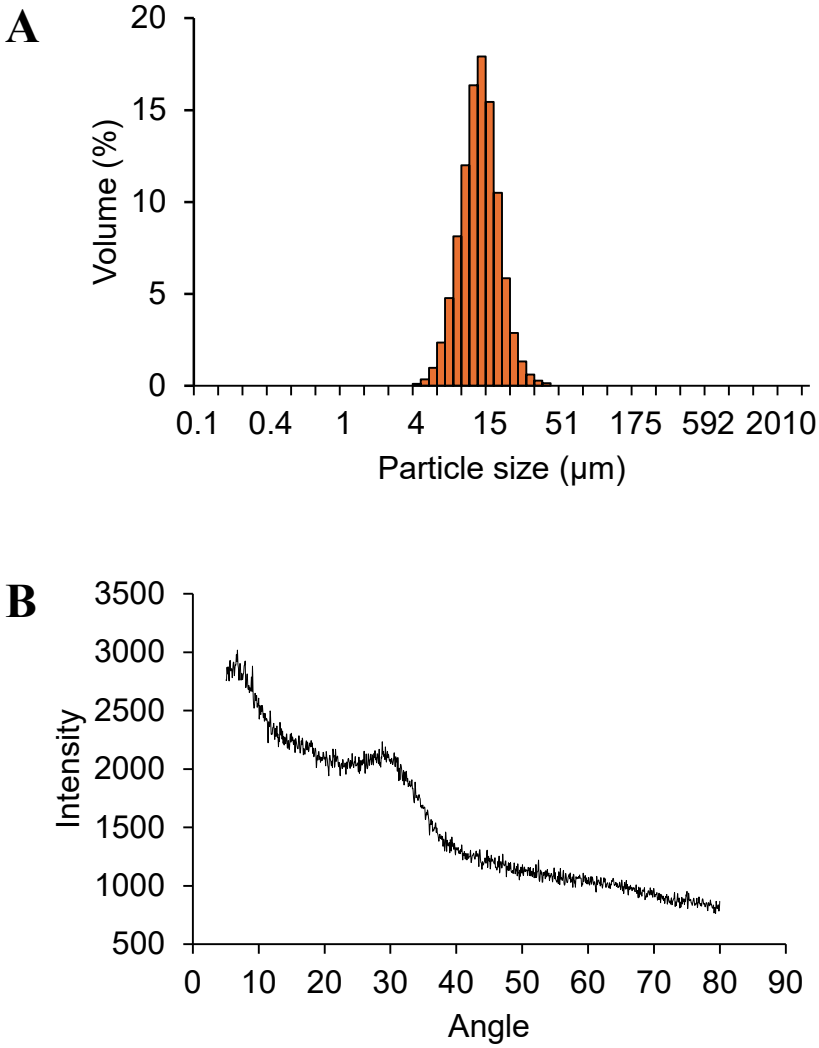


**Figure 24. Particle size distribution (A) and X-ray diffraction patterns (B) of RG.**

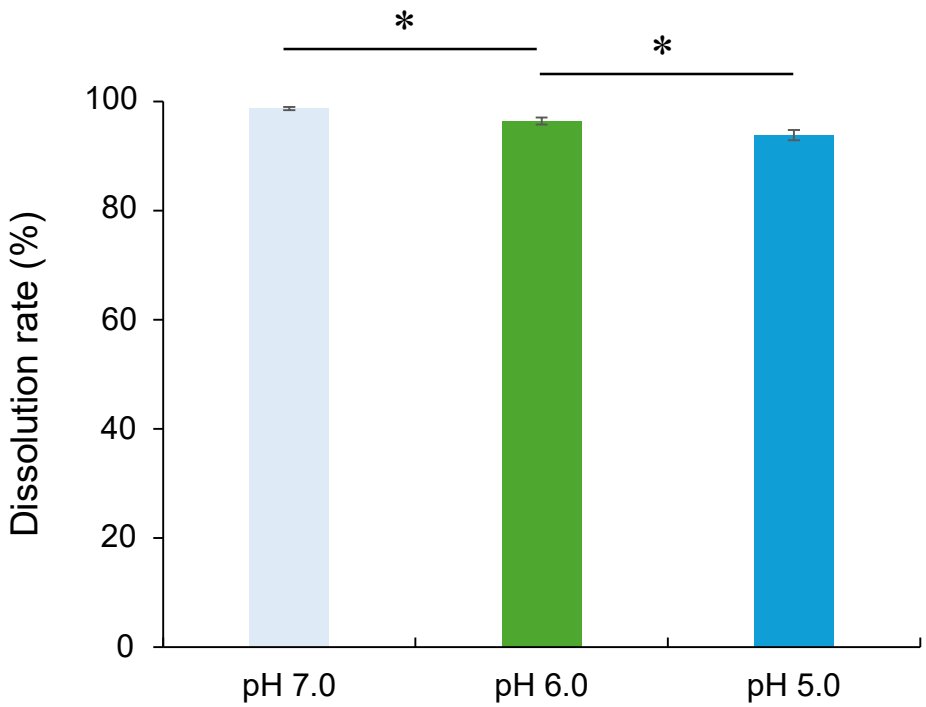


**Figure 25. Solubility of RG in the pH-adjusted buffer solution (pH 7.0, 6.0, or 5.0).** Bars represent the standard deviation of five replicates. * indicates significant differences ($p < 0.05$, ANOVA, Tukey's HSD test).

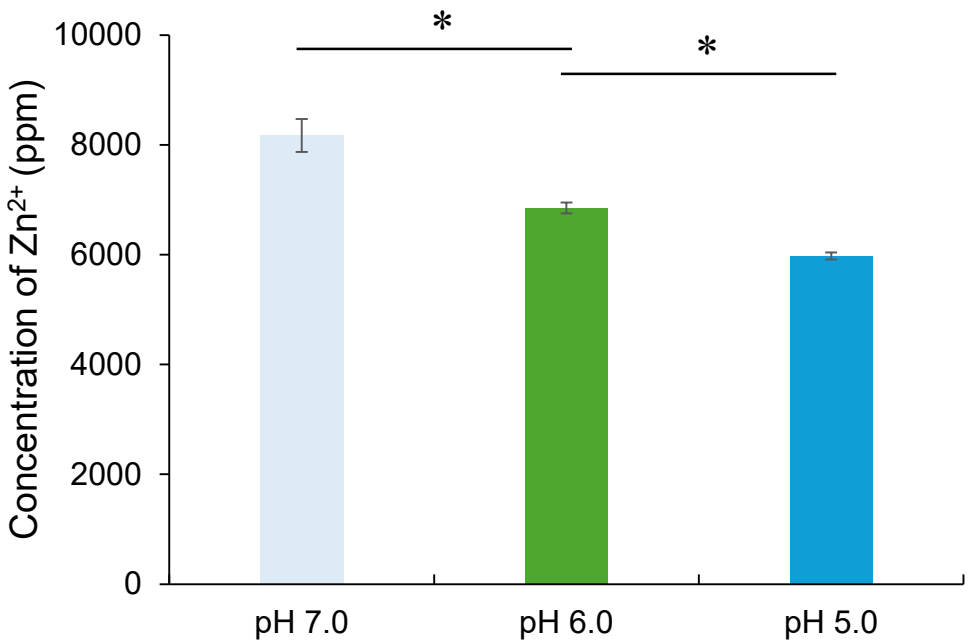


**Figure 26. Release of $Zn^{2+}$ from RG exposed to pH-adjusted BHI broth (pH 7.0, 6.0, or 5.0).** Bars represent the standard deviations of five replicates. * indicates significant differences ($p < 0.05$, ANOVA, Tukey's HSD test).

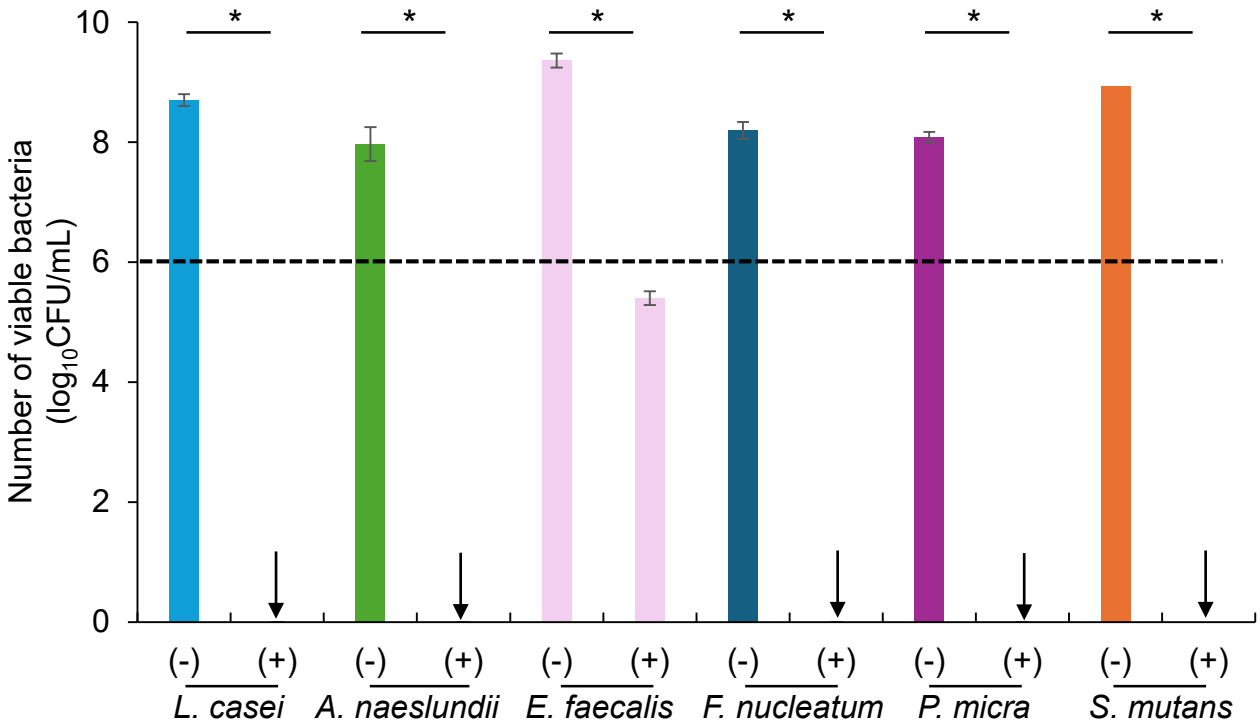


**Figure 27. Number of viable bacteria after incubation in the presence of RG.**

(-): After incubation in the absence of RG. (+): After incubation in the presence of RG. Arrows indicate 100% killing effect. Bars represent the standard deviations of five replicates. * indicates significant differences ($p < 0.05$, Student's *t*-test). Dashed line indicates the initial amount of bacteria.

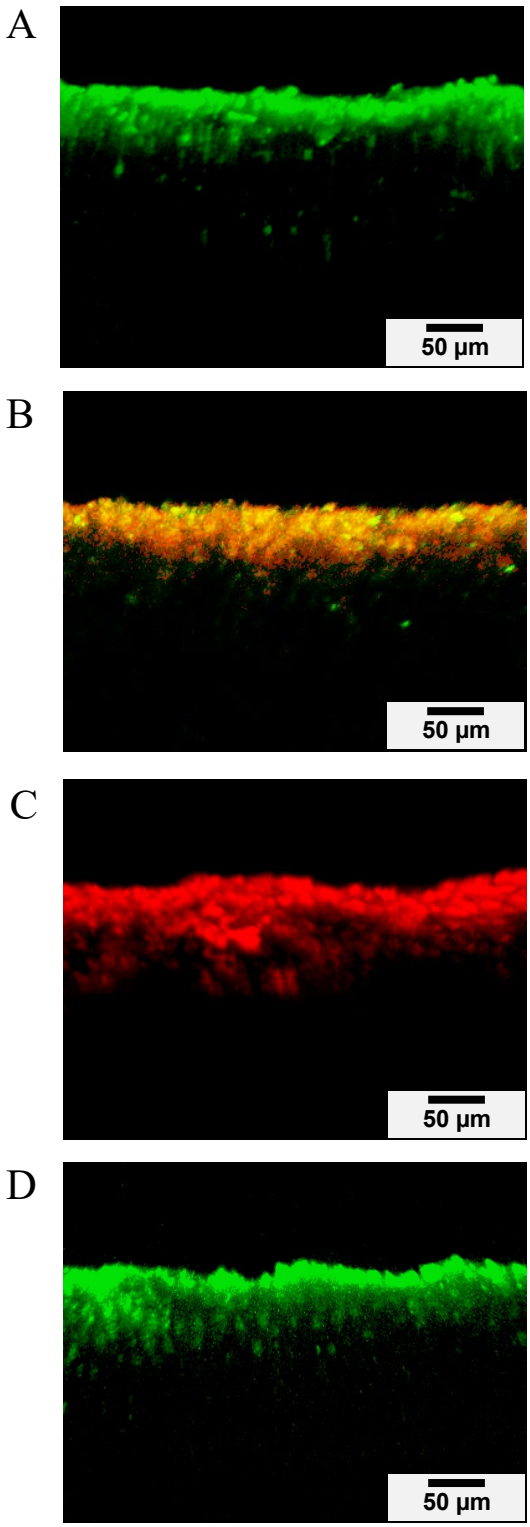


**Figure 28. CLSM images of *L. casei*-infected dentin model (A), *L. casei*-infected dentin model treated by dental resin incorporating 10 (wt)% RG under the dry condition (B), *L. casei*-infected dentin model treated by dental resin incorporating 10 (wt)% RG under the wet condition (C), and *L. casei*-infected dentin model treated by control resin without RG (D) after LIVE/DEAD staining.** Scale bar, 50 μm.

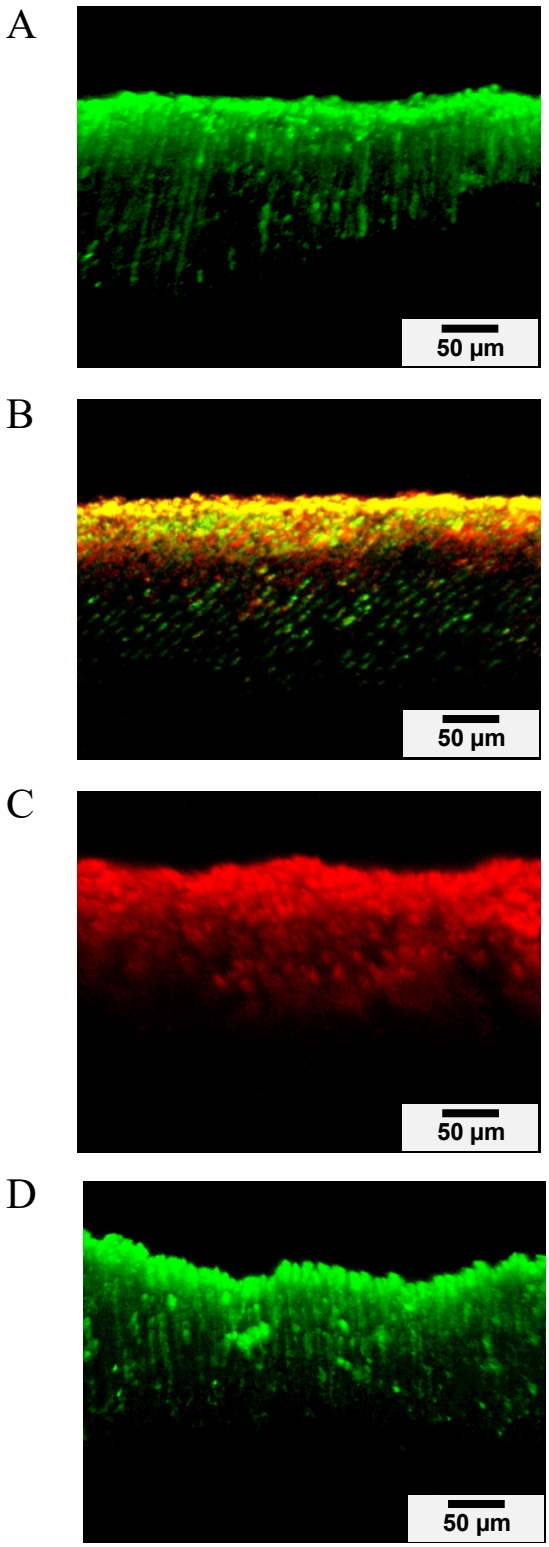


**Figure 29. CLSM images of *S. mutans*-infected dentin model (A), *S. mutans*-infected dentin model treated by dental resin incorporating 10 (wt)% RG under the dry condition (B), *S. mutans*-infected dentin model treated by dental resin incorporating 10 (wt)% RG under the wet condition (C), and *S. mutans*-infected dentin model treated by control resin without RG (D) after LIVE/DEAD staining.** Scale bar, 50 μm.